ISSN 0024-4902, Lithology and Mineral Resources, 2013, Vol. 48, No. 6, pp. 457–488. © Pleiades Publishing, Inc., 2013.
Original Russian Text © Yu.O. Gavrilov, E.A. Shcherbinina, O.V. Golovanova, B.G. Pokrovskii, 2013, published in Litologiya i Poleznye Iskopaemye, 2013, No. 6, pp. 522–551.

The Late Cenomanian Paleoecological Event (OAE 2) in the Eastern Caucasus Basin of Northern Peri-Tethys

Yu. O. Gavrilov[a, b], E. A. Shcherbinina[a], O. V. Golovanova[a], and B. G. Pokrovskii[a]

[a]*Geological Institute, Russian Academy of Sciences, Pyzhevskii per. 7, Moscow, 119017 Russia*
[b]*Faculty of Geology, Lomonosov Moscow State University, Moscow, 119991 Russia*
e-mail: gavrilov@ginras.ru, yugavrilov@gmail.com

Received May 13, 2013

Abstract—The Cretaceous sections of the eastern Caucasus contain rich in organic matter (OM) sediments corresponding to the late Cenomanian Oceanic Anoxic Event 2. They are marked by positive $\delta^{13}C$ and negative $\delta^{18}O$ isotopic anomalies, which are characteristic for this level in many areas of the world. The sediments exhibit distinct cyclic patterns reflected in an alternation of black OM-rich and gray more calcareous layers. The rocks are enriched with many chemical elements, although concentrations of some of them (Mo, Se) are lower than in typical sediments of anoxic basins. It is inferred that anoxic environments in the paleobasin were unstable and locally developed. Nannofossil assemblages from OAE 2 sediments are dominated by the highly resistant eurytropic taxon *Watznaueria* accompanied by common cool-water *Eprolithus* and rare warm-water *Rhagodiscus* representatives, which implies the development of environments unfavorable for the normal marine nannoflora and short-term cooling in the basin during OAE 2. The OM-rich sediments were deposited against the background of the rapid eustatic transgression due to a significant increase in productivity of phytoplankton in the paleobasin. The OAE 2 duration is estimated to be approximately 400 ka.

DOI: 10.1134/S0024490213060047

In many regions of the world, Cretaceous sections formed in oceans and epicontinental seas include rich in organic matter (OM-rich) sediments corresponding to the so-called global Oceanic Anoxic Events (OAEs) (Arthur and Schlanger, 1979; Arthur et al., 1987; Schlanger and Jenkins, 1976; Schlanger et al., 1987; and others). They are characterized by highly variable proportions of carbon and oxygen isotopes determined by changes in the carbon balance and global temperatures, wide development of oxygen-deficient (up to anoxic) environments, deposition of OM-rich sediments, and notable reorganizations in the taxonomic composition of the marine biota.

The Cretaceous sections of the northeastern Peri-Tethys, the eastern Caucasus included, also contain levels of OM-rich sediments , which are reliably correlated with most of the known OAEs (Gavrilov and Shcherbinina, 2005; Gavrilov et al., 2006; Shcherbinina et al., 2011; Shcherbinina and Gavrilov, 2012). The most remarkable among them is the event that occurred in the terminal Cenomanian (OAE 2), which is also termed as the Bonarelli Event.

Although OM-rich sediments reflecting this event are characterized by common features (enrichment in OM, considerable shifts in oxygen and carbon isotope ratios, significant variations in concentrations of trace elements, and others), they also exhibit distinct differences in their lithological–geochemical properties in different parts of the northeastern Peri-Tethys: high share of biogenic silica in some areas (western Caucasus, Georgia) and relatively high concentrations of carbonate material in others (Crimea, eastern Caucasus). Facies-variable sediments corresponding to the Bonarelli Event were investigated in the Cretaceous sections of the Crimea–Caucasus region (Alekseev et al., 1997; Bragina, 1999; Fischer et al., 2005; Gavrilov and Kopaevich, 1996; Gavrilov et al., 2009; Kopaevich and Kuzmicheva, 2002; Kuzmicheva, 2001; Naidin, 1993; Naidin and Alekseev, 1980; Naidin and Kiyashko, 1994a, 1994b; Shcherbinina and Aleksandrova, 2005; Tur, 1996). In many areas of the East European Platform, this level mostly corresponded to the hiatus (Alekseev et al., 1997; and others).

The purpose of this work is the complex sedimentological, geochemical, and paleontological (based on nannofossils) analysis of sediments corresponding to OAE 2 in Dagestan in order to interpret their depositional environments in the late Cenomanian basin of the eastern Caucasus, as well as to reveal their similar and specific features as compared with similar facies in different regions of the world.

In the course of study of OAE 2 sediments from Dagestan, we carried out extensive analytical investigations mostly in the Laboratory of Chemical-Analytical Investigations and Laboratory of Isotope Geochemistry and Geochronology (Geological Insti-

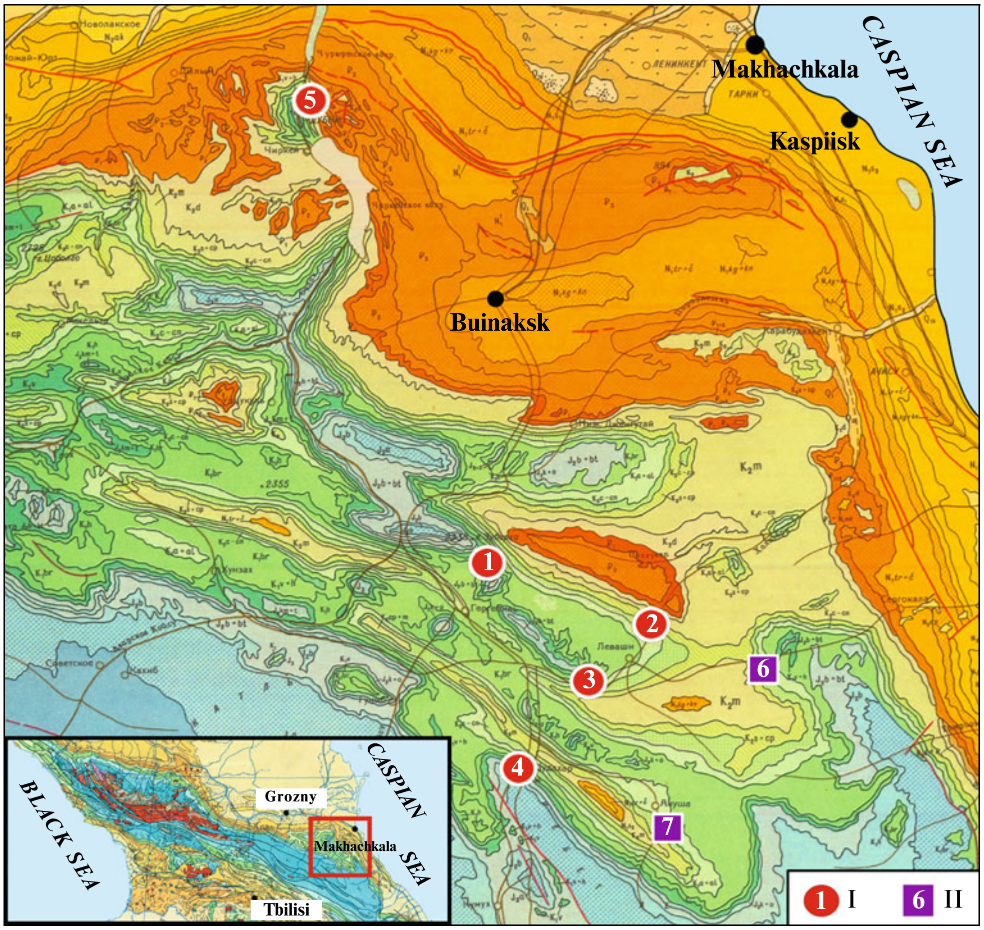

Fig. 1. Geological map of Dagestan with location of the OAE 2 sections. Inset shows the geological map of the Greater Caucasus; box designates the study area. (I) Location of examined OAE 2 sections: (1) Aimaki, (2) Levashi, (3) Khadzhalmakhi, (4) Karekadani (Tsudakhar), (5) Miatly HPP; (II) sections, where Turonian sediments cut OAE 2: (6) Levashi–Sergokala pass, (7) Akusha.

tute, Russian Academy of Sciences) with a S4 Pioner X-ray fluorescence spectrometer. Contents of C_{org} and CO_2 were analyzed by the chemical method (*Metody ...*, 1957).

Carbon and oxygen isotope compositions in carbonates were determined with the equipment designed by the Thermoelectron Corporation that included the Delta V Advantage spectrometer and Gas-Bench-II device. The samples and standards (KH-2, IAEA CO-1, and NBS-19) were decomposed using H_3PO_4 at temperature of 50°C. The $\delta^{13}C$ and $\delta^{18}O$ values are given in pro mille (‰) relative to the V-PDB standard. Accuracy (reproducibility) of $\delta^{13}C$ and $\delta^{18}O$ measurements was ±0.2‰.

The pyrolytic determination of OM was performed with a Rock-Eval 2 equipment at the Institute of Geology and Development of Combustible Mineral Resources.

POSITIONS OF OAE 2 SEDIMENTS IN SECTIONS OF CENTRAL DAGESTAN AND THEIR STRUCTURE

The member corresponding to the Bonarelli Event is traceable in several sections of Mountainous Dagestan: Aimaki, Levashi, Khadzhalmakhi, Karekadani (Tsudakhar) settlements, near the Miatly Hydroelectric Power Plant (hereafter, Miatly HPP), and other areas (Fig. 1).

It should be noted that these sections were formed in different depositional environments. Correspondingly, their structures and geochemical properties can also be different. Thus, these sections provide more complete information on their formation in different parts of the paleobasin.

The *Aimaki section* (Fig. 1, site 1) is stratigraphically most complete. The layer corresponding to OAE 2 occurs in the upper part of the Cenomanian section (Fig. 2). This section approximately 60 m thick is composed of irregularly alternating dark gray marl-

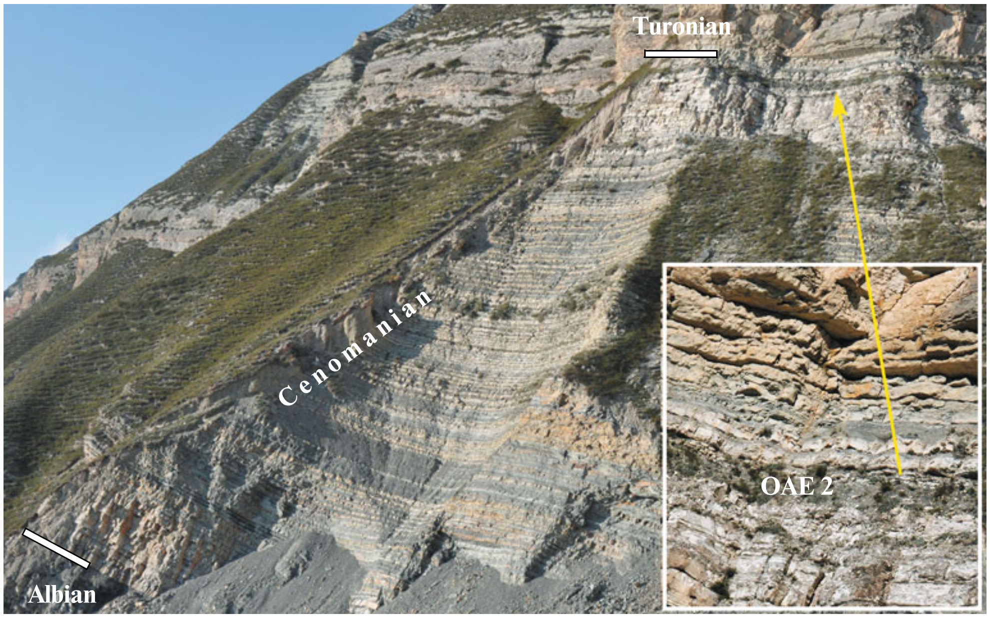

Fig. 2. Position of OAE 2 in the Cenomanian sequence of Aimaki section.

stones and limestones. Its basal, middle, and upper parts include members dominated by or completely composed of limestones. The Cenomanian section is characterized by the cyclic structure: it brings together two large sedimentation cycles similar in thickness and structure. The major cycles are in turn composed of smaller order cycles (at least two additional orders are definable) with thickness varying from one to several meters (Fig. 2).

The upper, limestone member (approximately 10 m thick, Fig. 3c) with the OAE 2 layer in the uppermost part represents the upper element of the second Cenomanian cycle of the eastern Caucasus. This member is composed of limestone layers with variable thickness and compactness. The limestones are compact, white to light gray, locally with pale yellow tint. The member includes several (at least 7 or 8) layers (1–8 cm thick) composed of dark gray clayey (smectite) material. Several levels in this member are marked by layers with siliceous (usually black) concretions.

The slightly uneven surface of the member of compact white limestones is overlain with a distinct boundary by a layer of gray (locally greenish gray) obscurely bedded clayey limestones 0.75–0.80 cm thick (Figs. 3a, 3b, 3d, 4) that are less compact than rocks of the underlying member. The terrigenous component includes glauconite grains (Fig. 5, samples 320-1, 320-2). At the middle part of this unit, the 0.15 m thick layer of relatively more compact light limestone occurs (Figs. 3d, 4; Layer 336-1). Together with the underlying clayey limestone it can be considered as a sedimentary cyclite, while the overlying bed of clayey limestone forms the lower part of the next (incomplete) cyclite. Rocks from this member differ lithologically from the underlying and overlying sediments. They are separated by distinct boundaries, the lower one likely corresponding to hiatus (Fig. 4d). Based on the integrity of features, it may be assumed that these sediments accumulated in relatively shallow-water depositional environments and included reworked underlying deposits. The similar member occurs in other coeval sections of Dagestan, although it is thinner (0.3–0.5 m) and lithologically uniform. The lithologically and stratigraphically similar sections with OAE 2 levels are known in in the Crimea (Aksudere and Sel'bukhra ones). In our opinion, this member likely reflects the initial sedimentation stage of the Bonarelli Event. Below, we term it as Layer α (Figs. 3, 4).

This member is overlain with a distinct boundary by the dark (locally almost black) OM-rich clayey–carbonate rocks termed as Layer β (Figs. 3–5; samples 322–327). In the Aimaki section, the Layer β is about 75–80 cm thick. As is shown below, organic matter from these sediments is dominated by sapropelic material that allows to identify it as Sapropelic Bed (SB). It is characterized by the layered structure: relatively massive dark gray sediments alternate with more with more tabular thinly-laminated varieties. While the fresh (unweathered) surface of black shales looks generally darker with insignificant color variations, their weathered surface demonstrates significantly more contrasting coloration of different layers. Thus, the SB structure is formed of different elementary cyclites (a pair consisting of a black shale layer grading upward into the paler calcareous rock). The SB includes 11 to 12 such cyclites (compare Figs. 3b and 3f).

The basal part of the SB and some of its inner levels are marked by lenticular or rounded sulfide concre-

Fig. 3. Positions of OAE 2 and host sequence in the Aimaki section. (a) Structure of sediments in the transitional Cenomanian–Turonian interval; triangles designate sedimentary cycles (length of the hammer in the oval is 35 cm); (α, β, γ) different layers of OAE 2 sediments; (b) sediments of Layer β (arrow indicates a pencil); (c) limestone member underlying the OAE 2 sediments (arrows indicate bentonite intercalations); (d) texture of Layer α; (e) siliceous concretion (black) (~0.5 m across) in limestone of Layer γ; (f) weathered OAE 2 rocks with the cyclic texture of the SB seen at the surface (cyclic patterns are vague on the "fresh" surface, see b).

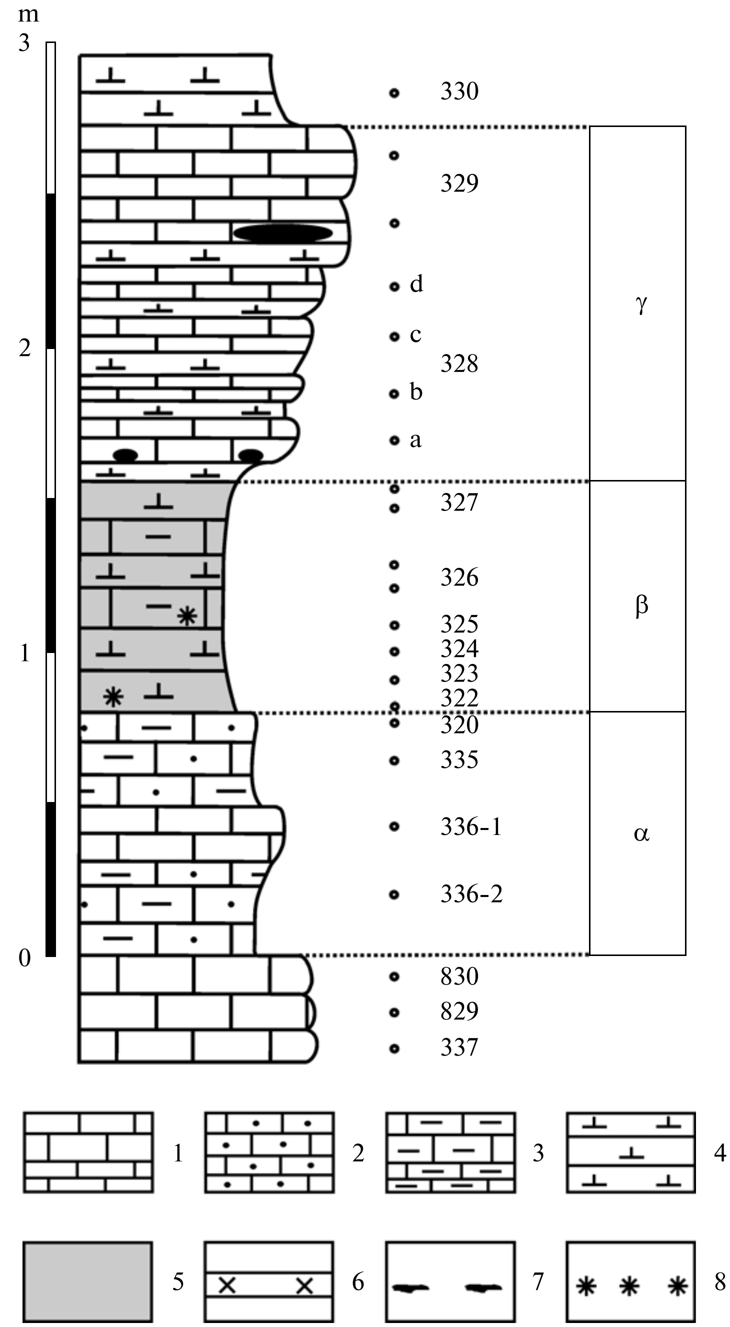

Fig. 4. Structure of the sedimentation cycle corresponding to OAE 2 and position of the carbonaceous member. Ciphers correspond to sample numbers; (α, β, γ) different parts of the sedimentary cycle. (1) Limestone; (2) sandy limestone; (3) clayey limestone; (4) marlstone; (5) carbonaceous sediments; (6) bentonite intercalations; (7) siliceous concretions; (8) pyrite concretions.

tions. Some bedding surfaces bear fish scales and are disturbed by fucoids *Chondrites*.

The 65 cm-thick interval overlying the SB is composed of alternating compact limestone 10–12 cm thick and softer marlstone (a few centimeters thick), which form Layer γ (Figs. 3a, 4). The lower layer contains small (a few centimeters across) black siliceous concretions. The rocks from this interval exhibit bioturbation features: large in limestones and smaller but more abundant in marlstone layers (samples 328a–328d). This interval is overlain by limestones (~0.5 m thick) with a bed (17 cm thick) of large lenticular black siliceous concretions up to 0.5 m in diameter (Figs. 3e, 4; Sample 329). The base and top of this bed are locally uneven, which is probably explained by redistribution of silica.

Layer α, carbonaceous clayey–carbonate sediments (Layer β), and the overlying limestone with a

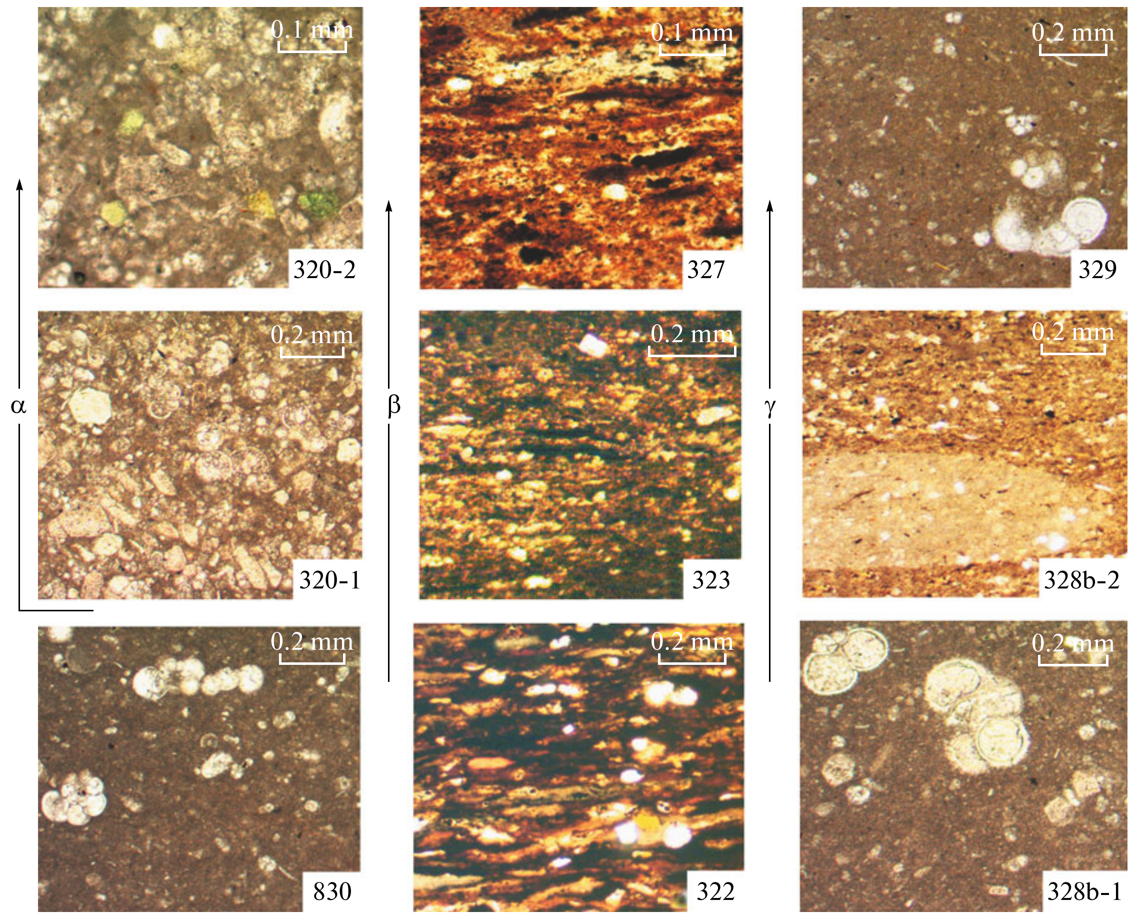

Fig. 5. Photomicrographs of rocks from different parts of the OAE 2 sediments in the Aimaki section. (830) Limestone from the top of the member immediately underlying the OAE 2 sediments; (320-1) rocks from Member α with glauconite inclusions (2); (322–327) high carbonaceous rocks from Member β; (328–329) clayey limestones and marls in Member γ (small light lens in photomicrograph 328b represents fucoid).

bed of black siliceous concretions (Layer γ) form the sedimentary cyclite (Fig. 4), which is structurally similar to other cyclites readily recognizable in Cenomanian sections of the eastern Caucasus (Fig. 2). Thus, the cyclite with OM-rich sediments consists of three parts corresponding to three stages of its formation. The lower part (Layer α) reflects the initial stage: accumulation of sediments during the lower sea level stand in relatively shallow-water depositional environments. OM-rich sediments (Layer β) were deposited during the rapid sea level rise and corresponding transgression. The upper part of the cyclite (Layer γ) was formed under conditions of the relatively stable sea level with the subsequent lowering at the terminal stage of the cyclite formation.

This cyclite is overlain by a member of alternating thickness-variable limestones and clayey–marly rocks (~5 m thick), which is, in turn, replaced upward by a sequence of massive middle Turonian limestones that form a distinct scarp in the topography (Figs. 2, 3a). This sequence is also composed of two sedimentary cyclites: (1) lower thin cyclite consisting of alternating layers (a few centimeters thick) of more and less compact clayey limestones (0.4 m) and overlying limestone (0.5 m); (2) upper, thicker (3.5 m thick) cyclite composed of clayey marlstone in the lower part, thin limestone laminae in the middle part, and a compact limestone 0.4 m thick at its top. It is conceivable that the basal bed (0.7 m thick) of the Turonian limestone sequence also belongs to this cyclite. As is shown below, the Cenomanian/Turonian boundary is located at the level of Sample 331-1, i.e., within the upper part of this sedimentary cyclite.

Levashi, Khadzhalmakhi, and Karekadani sections (Fig. 1, sites 2–4). The Levashi section (near the road between the Levashi and Khadzhalmakhi settlements) and the Karekedani section (near the large Tsudakhar Settlement) demonstrate general similarity with the Aimaki section (Figs. 6, 7a–7d). At the same time, unlike rocks in the Aimaki area, limestones of these sections onlap the SB with a distinct erosion surface. Thus, several meters thick of the upper Cenomanian sediments overlying the SB observed in the Aimaki section are eroded. The 0.3–0.5 m thick Layer α in these sections is readily definable. The weathered surface of the SB demonstrates well-developed cyclic pat-

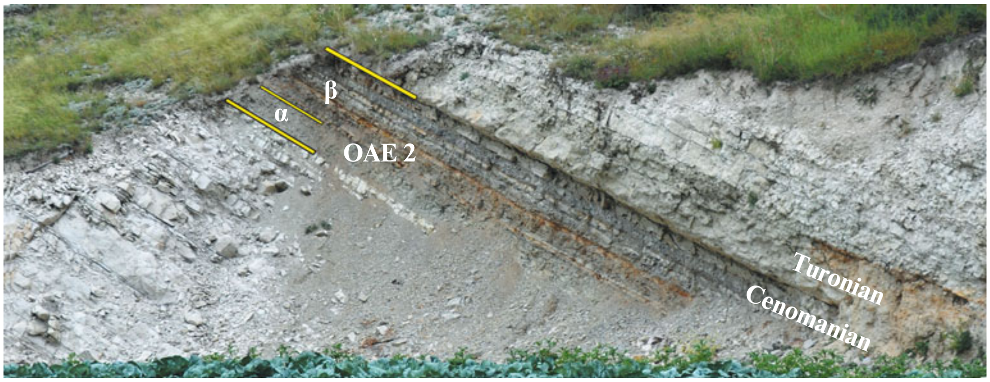

Fig. 6. OAE 2 sediments in the transitional Cenomanian/Turonian interval of the Levashi section.

terns (Figs. 6, 7b, 7d). The underlying limestones enclose several layers of bentonite.

Thus, OM-rich sediments over the most area of the eastern Caucasus region (Aimaki, Levashi, Karekadani, and Khadzhalmakhi sections) are characterized by a well-developed cyclic structure: thickness of cyclic bands varies from 3 or 4 to 10–15 cm (rarely, more). Each band includes 11 or 12 cyclites (Figs. 6, 7b, 7d). The basal part of each cyclite is usually composed of dark sediments highly enriched in OM, while its upper part is represented by gray more calcareous rocks. Transition between the lower and upper elements of the cyclites is usually rather distinct and relatively gradual, while boundaries between individual cyclites are usually sharp. Judging from the description of the OAE level in (Tur, 1996), similar cyclic patterns of sediments are also characteristic of sections in westerly areas of the northeastern Caucasus (for example, the Bass section in Chechnya). Such bedding patterns of lithologically different members are also observable in other areas of the world. For example, the cyclicity determined by fluctuations in the C_{org} and $CaCO_3$ concentrations is recorded in the Bonarelli Event sediments from the Turfaya basin on the Atlantic coast of Morocco (Kuhnt et al., 1997) and other areas.

Miatly HPP section (Fig. 1, Site 5; Figs. 7e, 7f). Among all Cretaceous sections exposed in Dagestan, it occupies the northernmost position and crops out in the core of the Khadum anticline. The Cenomanian section in this area notably differs from its southerly counterparts. First, its thickness is significantly reduced (approximately 10 m). Second, it is dominated by limestones: the basal Cenomanian layer (up to 2.5–3.0 m thick) is overlain by a limestone member (0.2–0.6 m thick) with layers of black marlstones (10–20 cm) in its upper part (Fig. 7f). Some limestone layers are gray-brown due to admixture of OM. The rocks are compact due to intense postdiagenetic alterations caused by the elevated heat flow in this area. These processes intensified the effect of microfossil recrystallization in limestones. The lower and upper boundaries of the OAE 2 member are vague in this section. Nevertheless, it is undoubted that OAE 2 includes the black marlstone layer (~20–25 cm thick), which is highly enriched in OM and marked by sulfide concretions 2–3 cm in diameter, and several overlying limestone layers. This is evident from the most intense peak of the carbon isotope anomaly. The bedded Cenomanian sequence is overlain by massive Turonian limestones (Fig. 7e).

It should be noted that the Cenomanian sections in the pass between the Levashi and Sergokala settlements and in the section near the Akusha Settlement lack the OAE 2 sediments due to erosion during the early Turonian regression (Fig. 1, sites 6 and 7).

Distribution of bentonite layers in Cenomanian sections. The Cretaceous sections of the eastern Caucasus enclose relatively abundant bentonite intercalations, which are irregularly scattered along the section. The number of such layers is maximum in the Campanian interval, but they are also abundant in the Cenomanian sequence. In the Aimaki section, two layers up to 10–15 cm thick occur in the limestone member in its middle part (i.e., in the upper part of the large lower cycle), although their highest number (7 to 8) is confined to the limestone member underlying OAE 2 sediments in the uppermost Cenomanian interval (Fig. 3c). They are also recorded in the Turonian sequence. The quantitative distribution of bentonite intercalations in the section implies volcanic activation in the late Cenomanian in the period preceding the Bonarelli Event. Many researchers of the Bonarelli Event in other regions note the presence of bentonite intercalations in sequences enclosing OAE 2 sediments (Prokoph et al., 2001; Bowman and Bralower, 2005; and others). Although volcanic activity at that time was worldwide (Hays and Pittman, 1973; Kerr, 1998; Kuroda et al., 2007; Sinton and Duncan, 1998; and others), ash was likely transported to the eastern Caucasus from zones with intense volcanism in the Transcaucasus region,

Fig. 7. OAE 2 sediments in the transitional Cenomanian–Turonian interval of different sections. (a, c, e) Positions of the OAE 2 sediments in sections: (a) Khadzhalmakhi, (c) Karekadani (Tsudakhar), (e) Miatly HPP; (b, d, f) structures of the OAE sediments in the corresponding sections; in photo d, the field notebook is 10 × 15 cm in size; in photo f, pyrite concretion is 3 cm in diameter.

where thick volcanosedimentary sequences were formed at that time (*Geologiya* ...., 1970, 1972)

STRATIGRAPHY OF THE UPPER CENOMANIAN–LOWER TURONIAN SEQUENCES IN DAGESTAN BASED ON NANNOFOSSILS

The taxonomic composition of nannofossil assemblages in the transitional Cenomanian–Turonian sediments was examined in the Aimaki, Levashi, and Karelkadani sections. Abundance of nannofossils in different facies of this stratigraphic interval is highly variable and their preservation ranges from moderate to poor (mostly in compact limestones). Nevertheless, their assemblages appeared to be sufficiently representative for the zonal subdivision of sections using the nannofossil biostratigraphic scales.

The sequence under consideration is referred to the upper Cenomanian–lower Turonian interval corresponding to CC10–CC12 zones in the scale proposed in (Sissingh, 1977; Perch Nielsen, 1985) or UC5–UC8 zones in the scale proposed in (Barnett, 1998). The main nannofossil events of this interval are: last appearance (LA) of *Lithraphidites acutus* and *Axopodorhabdus albianus* that mark the lower boundaries of UC5 and UC5b zones, respectively (Fig. 8); first appearance (FA) of *Quadrum intermedium* at the base of the UC5c Zone; LA of *Helenea chiastia* corresponding to the Cenomanian/Turonian stage or CC10a/CC10b (=UC5/UC6) boundary; FA of *Quadrum gartneri* at the CC10/CC11 (=UC6/UC7) boundary; FA of *Eiffelithus eximius* that marks the lower boundary of the CC12 (=UC8) Zone and the base of the middle Turonian Substage.

In the Aimaki section, LA of *Lithraphidites acutus* is documented immediately below the scarp of compact limestones that constitute the base of the interval considered in this paper, which allows the UC4/UC5 boundary to be placed ~8 m below the SB base. The LA of *Axopodorhabdus albianus*, a rare species in this basin, recorded in the Aimaki section 3.6 m below the SB marks the UC5a/UC5b subzone boundary (Fig. 9). In the Levashi and Karekadai sections, this level is located 3 and almost 8 m below the SM, respectively. This species is characterized by asynchronous LA in the Tethyan and Boreal realms. For example, its LA coincides with the level specified in the Barnett's scale in the southern Bohemian basin (Cech et al., 2005) and Italy (Luciani and Cobianchi, 1999), whereas its LA precedes the LA of *L. acutus.* in the classical English Eastbourne section (Paul et al., 1999), Spain (Lamolda et al., 1997), Vocontian basin in France (Fernando et al., 2010), and Romania (Melinte-Dobrinerscu and Bojar, 2008).

The FA of *Quadrum intermedium* at the base of the UC5c Subzone in the Aimaki, Levashi, and Karekadani sections is recorded approximately 3.0, 2.3, and 10.7 m, respectively, below the SB. The FA of this species in the sections under consideration is close to the level accepted in the Barnett's scale (Fig. 8), although *Q. intermedium* appears higher in some sections of the world: in the lower Turonian UC6 and UC7 zones (Hardas and Mutterlose, 2006; Luciani and Gobianchi, 1999; Paul et al., 1999). In the UC5c Subzone of central Dagestan, we have established several LAs of nannofossil species, which mark boundaries between the subzones of earlier zonal units in the Barnett's scale. For example, *Corolithion kennedyi*, whose LA should mark the lower boundary of the UC3e Subzone in the lower part of the upper Cenomanian, continues to exist in Dagestan sections in higher levels reaching the UC5c Subzone, closely to the level of its LA in the Vocontian basin in France (Fernando et al., 2010). Higher levels of LAs of this species are recorded in Italy (above the Bonarelli Event) (Luciani and Cobianchi, 1999) and in western Crimea (Sel'bukhra section, original data). According to Barnett scale, *Rhagodiscus asper* demonstrates its LA in the UC5b Subzone. This species occurs up to the terminal part of the UC5c Subzone in section, disappears at the base of the UC7 (=CC11) zone in California (Fernando et al., 2011), continues to exist in the lower Turonian interval above the *Quadrum gartneri* FA in Egypt (Tantawi, 2008), and is reported from the middle Turonian Substage (above the FA of *Eiffelithus eximius* in the Vocontian basin (Fernando et al., 2010). The last appearance of *Gartnerago nanum* marks the base of the UC3d Subzone. It occurs sporadically in sections under consideration up to the UC5c Subzone, where its LA coincides with the FA of *Eprolithus octopetalus.* According to the Barnett scale, the latter species should appear in the UC5c Subzone (below the *H. chiastia* disappearance). It appears in sediments of this interval in Morocco (Tantawi, 2008), Bohemian basin (Čech et al., 2005), Crimea, and eastern Caucasus. The close appearance level is characteristic of this species in sections of Spain (Lamolda et al., 1997) and Romania (Melinte-Dobrinescu and Bojar, 2008). As in the Crimean sequences, *E. octopetalus* appears in the Aimaki section immediately below the SB. In many sections of the world, its FA is recoded higher: at the base of the Turonian (CC11 Zone) (Fernando et al., 2010; Hardas and Mutterlose, 2006; Luciani and Cobianchi, 1999). *Lucianorhabdus* sp. nannoliths (Fig. 10) documented in the middle part of the UC5c Subzone likely represent the oldest known finds of this taxon: up to date, first representatives of this evolutionary lineage were found in the UC6b Subzone sediments of the Bohemian basin (Čech et al., 2005).

The LA of *Helenea chiastia* corresponding to the CC10a/CC10b (=UC5/UC6) boundary and representing the closest to the Cenomanian/Turonian boundary nannofossil event (Kennedy et al., 2005) is documented in the Aimaki section approximately 3.2 m above the sole of SB (Figs. 8, 9; Sample 331b).

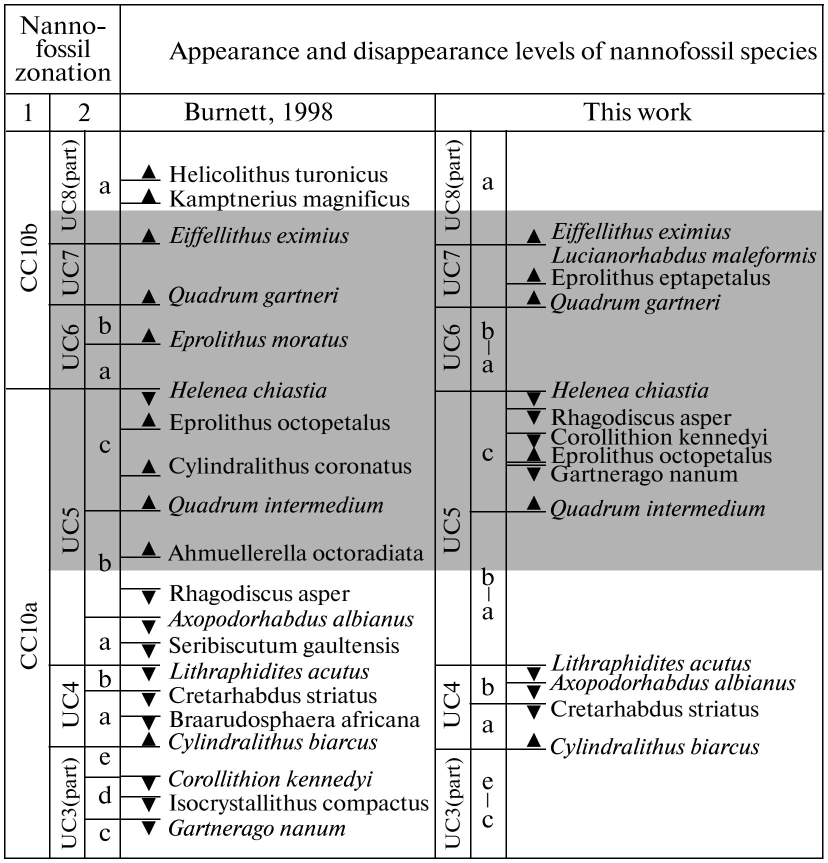

Fig. 8. Chart showing Sissingh (1) and Burnett (2) zonal scales, correlation of FAs and LAs of nannofossil species accepted in the Burnett scale and in sections of central Dagestan (this work). Italic designates primary markers; (a–f) nannoplankton subzones; the interval discussed in this work is gray-colored.

The thin interval of the lower Turonian UC6 Zone (=CC10b Subzone) is marked by the FA of *Eprolithus eptapetalus* (=*E. moratus*) only that corresponds to the base of the UC6b Subzone. Its presence at this level (prior to the *Quadrum gartneri* FA) takes place in Germany (Linnert et al., 2010), England (Burnett, 1998), and California (Fernando et al., 2011). In the Dagestan sections, this species appears together with *Quadrum gartneri* at the base of the UC7 Subzone. In the Vocontian basin, its FA is noted even higher, in the middle Turonian UC8 Zone (above the FA of *Eiffelithus eximius*).

In the Aimaki section, the *Quadrum gartneri* FA (base of the CC11 (=UC7) Zone), which was previously accepted as a marker of the Cenomanian/Turonian boundary (Tsikos et al., 2004; and others) is recognized 5.6 m above the SB base.

Eiffelithus eximius and *Lucianorhabdus maleformis* that mark the middle Turonian CC12 (=UC8) Zone appear 0.4 m above the FA of *Q. gartneri*. In the Levashi and Karekadani sections, these species are recorded in the compact yellowish pink limestones onlapping along the erosional surface upon the SB. Despite the fact that the Aimaki section includes the most complete lower Turonian interval among the examined successions, its small thickness (1.7 m) indicates likely condensed sedimentation. The simultaneous FAs of *E. eximius* and *L. maleformis*, which coincides with the unexpectedly early appearance of first *Micula* representatives, implies likely short hiatus at the base of the middle Turonian. Their similar early appearance is established in the western Crimean sections, while representatives of this genus are usually characteristic of the Coniacian.

Thus, the central Dagestan sections demonstrate successive FAs and LAs of the primary and secondary zonal nannofossil markers, which provide grounds for defining all zonal units of the standard nannofossil

Fig. 9. Nannofossil zonation of the Cenomanian/Turonian transition of the Aimaki section and levels of the FAs and LAs of most common nannofossil species. (1) Zones according to (Sissingh, 1977); (2) zones according to (Burnett, 1988); the SB is gray-colored; the entire OAE 2 interval is shaded.

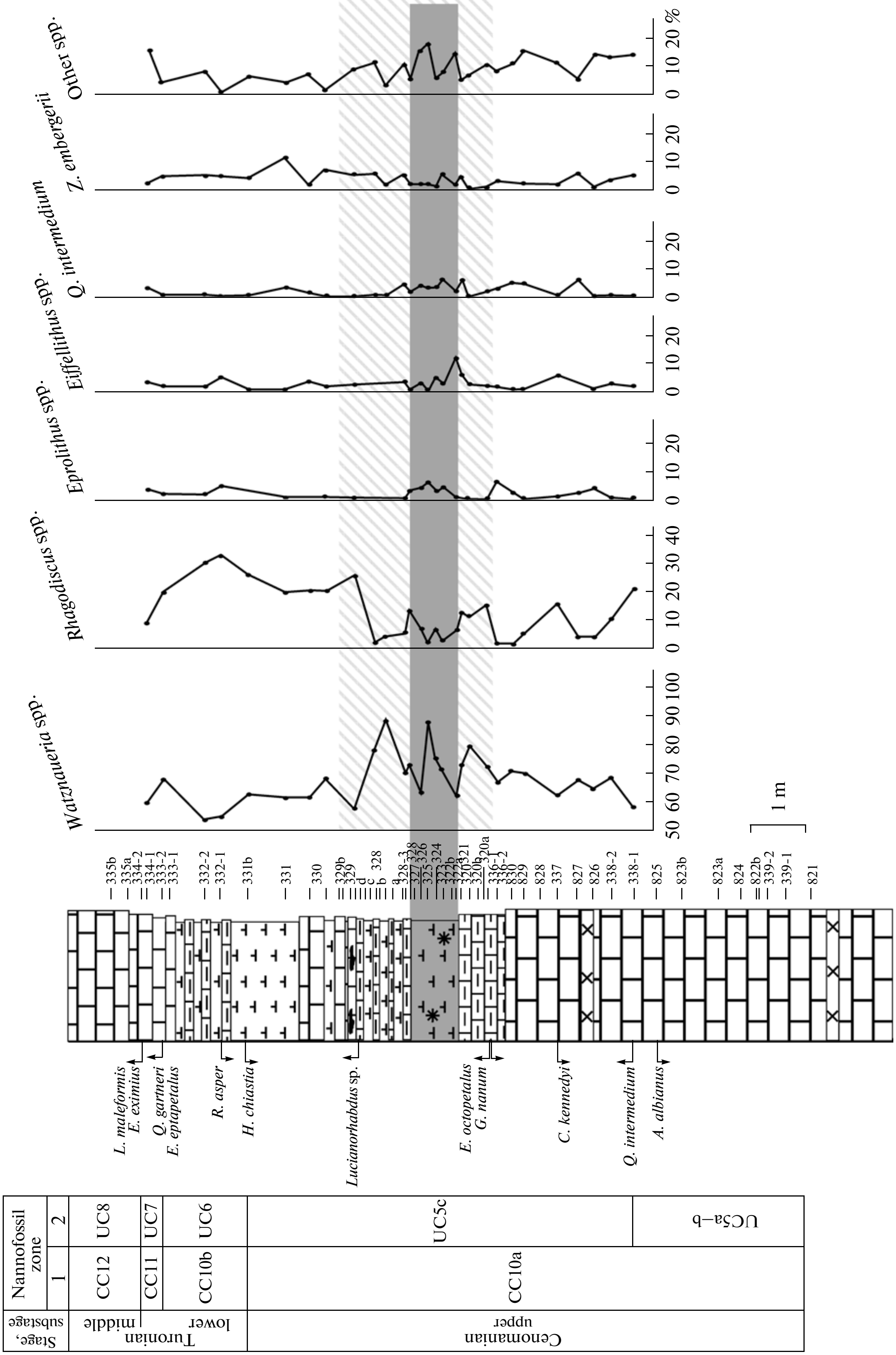
Watznaueria spp.
Rhagodiscus spp.
Eprolithus spp.
Eiffellithus spp.
Q. intermedium
Z. embergeri
Other spp.
%
1 m
L. maleformis
E. eximius
Q. gartneri
E. eptapetalus
R. asper
H. chiastia
Lucianorhabdus sp.
E. octopetalus
G. nanum
C. kennedyi
Q. intermedium
A. albianus
Nannofossil zone
Stage, substage
Turonian
middle
lower
Cenomanian
upper
CC12
CC11
CC10b
CC10a
UC8
UC7
UC6
UC5c
UC5a–b

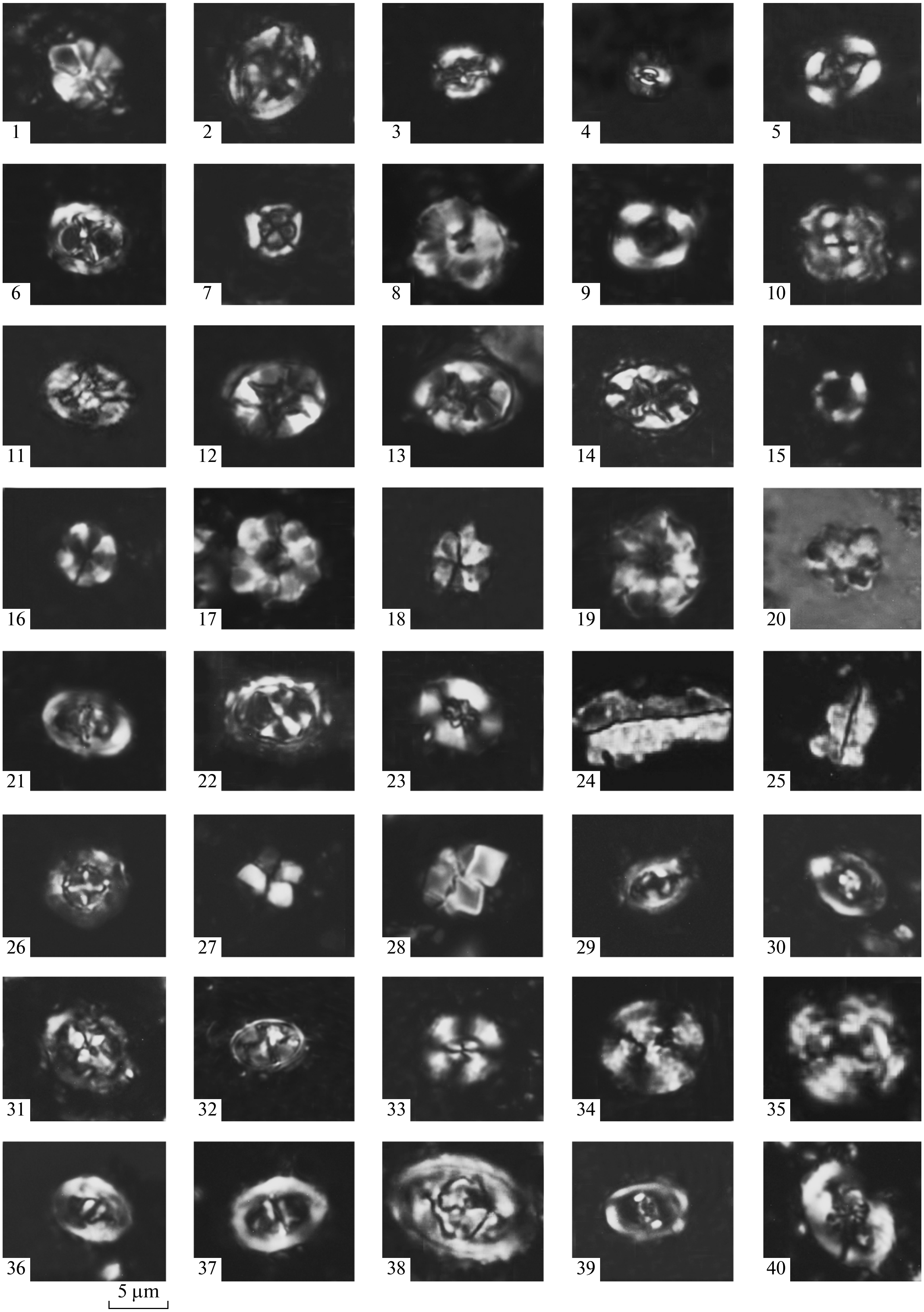
1
2
3
4
5
6
7
8
9
10
11
12
13
14
15
16
17
18
19
20
21
22
23
24
25
26
27
28
29
30
31
32
33
34
35
36
37
38
39
40
5 μm

scales in the transitional Cenomanian–Turonian interval and show the stratigraphic position of the SB in the UC5c Subzone (=upper part of the CC10a Subzone) of the terminal Cenomanian.

LITHOLOGICAL AND GEOCHEMICAL DESCRIPTION OF THE OAE 2 SEDIMENTS

Organic matter and $CaCO_3$ in the upper Cenomanian sections

The most characteristic feature of the SB sediments is their enrichment with organic matter: C_{org} amounts to 7–9% (Figs. 11–15). Moreover, this enrichment is rapid and confined to the sharp boundary with the underlying rocks. At the same time, as was noted above, the OM distribution in OAE 2 sediments is very irregular, which is explained by their cyclic patterns: lower elements of cyclites are highly enriched with OM against the background of relatively low $CaCO_3$ concentrations, while the $CaCO_3$ content notably increases and the C_{org} content decreases (down to <1%) in upper elements.

The OAE 2 sediments with the best developed cyclic patterns (Khadzhalmakhi and Karekadani sections, Fig. 7) demonstrate clearly that the thickness of cyclites increases upward the section from 4 or 5 to 12–15 cm. Simultaneously, the thickness of OM-rich layers increases upsection from 1.0–1.5 to 5–10 cm. The maximal C_{org} concentrations are recorded in the thickest cyclites in the upper half of the member. It should be noted that differences between the lower and upper elements of cyclites in this interval can be smoothed; i.e., differentiation of carbonaceous and carbonate material becomes less distinct owing to the high organic matter content in the entire cyclite section. In the uppermost part of the OAE 2, the thickness of cyclites again decreases, while difference between their elements increases.

It should be noted that some levels in the sequence hosting the OAE 2 sediments are also enriched in organic matter. For example, the upper Cenomanian Khadzhalmakhi and Karekadani sections include marlstone or clayey limestone layers with the maximal C_{org} content reaching 2 to 3% (Figs. 13, 14). The Aimaki section, where one can see the C_{org} distribution in sediments overlying the carbonaceous member, some layers contain as much as 2% organic carbon (Fig. 11). This interval encloses a limestone bed with lenses of early diagenetic black siliceous concretions. Their black color is related to the presence of dissolved OM in interstitial water at the diagenetic stage. Therefore, it is conceivable that even limestone beds, where the C_{org} concentration is minimal now or lacking it at all, contained initially some OM that was subsequently oxidized (mostly, at the diagenetic stage). Therefore, its concentration in sediments appeared to be reduced up to complete disappearance.

Organic matter in the upper Cenomanian sediments is present in different forms. Transparent thin sections of samples from OM-rich sediments demonstrate that it is dominated by structureless aggregates corresponding to colloalginite, according to the classification by (Ginsburg, 1991). Often, OM forms thin laminae and small flattened lenses (from hundredths part of a millimeter to several millimeters long) arranged parallel to bedding surfaces (Fig. 5,

Fig. 10. Photomicrographs of nannofossil species from the transitional Cenomanian–Turonian interval of central Dagestan. All images (with the exception of photomicrograph 20) are obtained in the polarized light. (1) *Assipetra terebrodentarius* (Applegate et al. in Covington and Wise, 1987); Rutledge and Bergen in Bergen, 1994, Levashi section, sample 1003); (2) *Axopodorhabdus albianus* (Black, 1967; Wind and Wise in Wise and Wind, 1977, Levashi section, sample 1003; (3) *Acaenolithus cenomanicus* Black, 1973, Karekadani section, sample 3-1; (4) *Biscutum constans* (Górka, 1957): Black in Black and Barnes, 1959, Aimaki section, sample 338; (5) *Broinsonia signata* (Noël, 1969) Noël, 1970, Levashi section, Sample 1001; (6) *Chiastozygus platyrhethus* Hill, 1976, Karekadani section, sample 4-1; (7) *Corollithion kennedyi* Crux, 1981, Aimaki section, sample 826; (8) *Cylindralithus nudus* Bukry, 1969, Levashi section, Sample 178a; (9) *Cylindralithus sculptus* Bukry, 1969, Aimaki section, Sample 338; (10) *C. sculptus*, Levashi section, sample 1005; (11) *Eiffellithus eximius* (Stover, 1966) Perch-Nielsen, 1968, Aimaki section, sample 334; (12) *Eiffellithus turriseiffeli* (Deflandre in Deflandre and Fert, 1954) Reinhardt, 1965, Aimaki section, sample 332-1; (13) *Eiffellithus digitatus* Shamrock, 2009, Aimaki section, sample 334; (14) *Eiffellithus* sp., Aimaki section, sample 338; (15) *Eprolithus apertior* Black, 1973, Aimaki section, sample 334;(16) *Eprolithus floralis* (Stradner, 1962) Stover, 1996, Levashi section, sample 1003; (17) *E. floralis*, Levashi section, sample 178a; (18) *Eprolithus octopetalus* Varol, 1992, Levashi section, sample 1001; (19) *Eprolithus eptapetalus* Varol, 1992, Levashi section, sample 182; (20) *Eprolithus eptapetalus*, Aimalki section, sample 334; (21) *Gartnerago nanum* Thierstein, 1974; Levashi section, sample 1001; (22) *Gartnerago chiasta* Varol, 1991, Karekadani section, sample 4-2; (23) *Helenea chiastia* Worsley, 1971, Karekadani section, sample 5-1; (24) *Lucianorhabdus maleformis* Reinhardt, 1966, Aimaki section, sample 334; (25) *Lucianorhabdus* sp., Aimaki section, sample 329b; (26) *Prediscosphaera columnata* (Stover, 1966) Perch-Nielsen, 1984, Karekadani section, sample 4-2; (27) *Quadrum gartneri* Prins and Perch-Nielsen in Manivit et al., 1977, Aimaki section, sample 333-1; (28) *Quadrum intermedium* Varol, 1992, Aimaki section, sample 333-1; (29) *Rhagodiscus achlyostaurion* (Hill, 1976) Doeven, 1983, Karekadani section, sample 3-2; (30) *Rhagodiscus asper* (Stradner, 1963) Reinhardt, 1967, Aimaki section, sample 333b; (31) *Rhagodiscus splendens* (Deflandre, 1953) Verbeek, 1977, Karekadani section, sample 4-2; (32) *Tranolithus orionatus* (Reinhardt, 1966a) Reinhardt, 1966b, Karekadani section, Sample 3-1; (33) *Watznaueria barnesiae* (Black in Black and Barnes, 1959); Perch-Nielsen, 1968, Levashi section, sample 1003; (34) *Watznaueria biporta* Bukry, 1969, Karekadani section, sample 4-2; (35) *Watznaueria manivitae* Bukry, 1973, Aimaki section, sample 329-1; (36) *Zeugrhabdotus bicrescenticus* (Stover, 1966) Burnett in Gale et al., 1996, Aimaki section, sample 333-1; (37) *Zeugrhabdotus diplogrammus* (Deflandre in Deflandre and Fert, 1954) Burnett in Gale et al., 1996, Aimaki section, sample 329-1; (38) *Zeugrhabdotus embergeri* (Noël, 1958) Perch-Nielsen, 1984, Levashi section, sample 1001; (39) *Zeugrhabdotus noeliae* Rood et al., 1971, Aimaki section, sample 829; (40) *Zeugrhabdotus scutula* (Bergen, 1994) Rutledge et Bown, 1996), Karekadani section, sample 3-1.

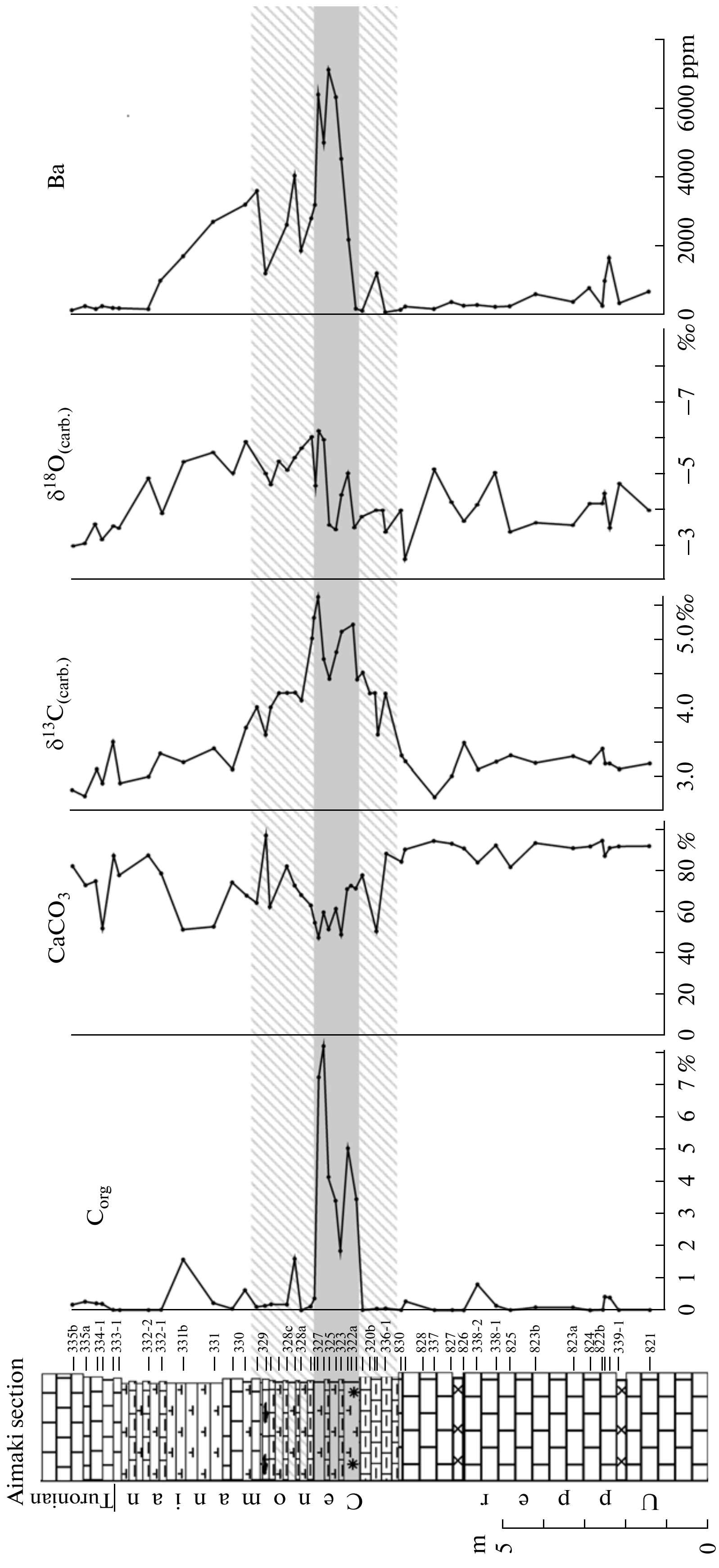

Fig. 11. Lithology of the transitional Cenomanian–Turonian sediments in the Aimaki section and distribution of C_{org}, $CaCO_3$, $\delta^{13}C$, $\delta^{18}O$, and Ba. For legend in Figs. 11–16, see Fig. 4.

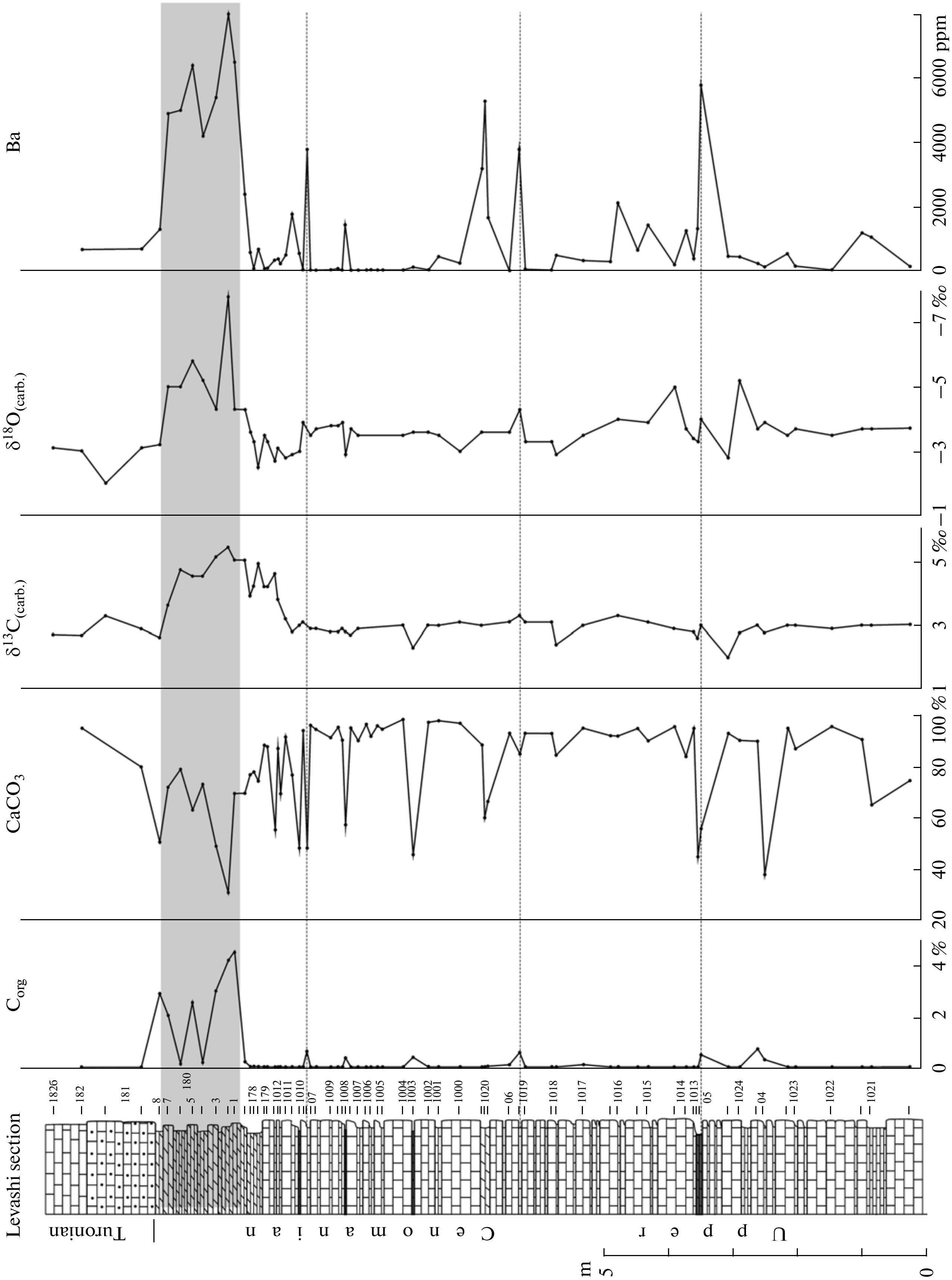

Fig. 12. Lithology of the transitional Cenomanian–Turonian sediments in the Levashi section and distribution of C_{org}, $CaCO_3$, $\delta^{13}C$, $\delta^{18}O$, and Ba.

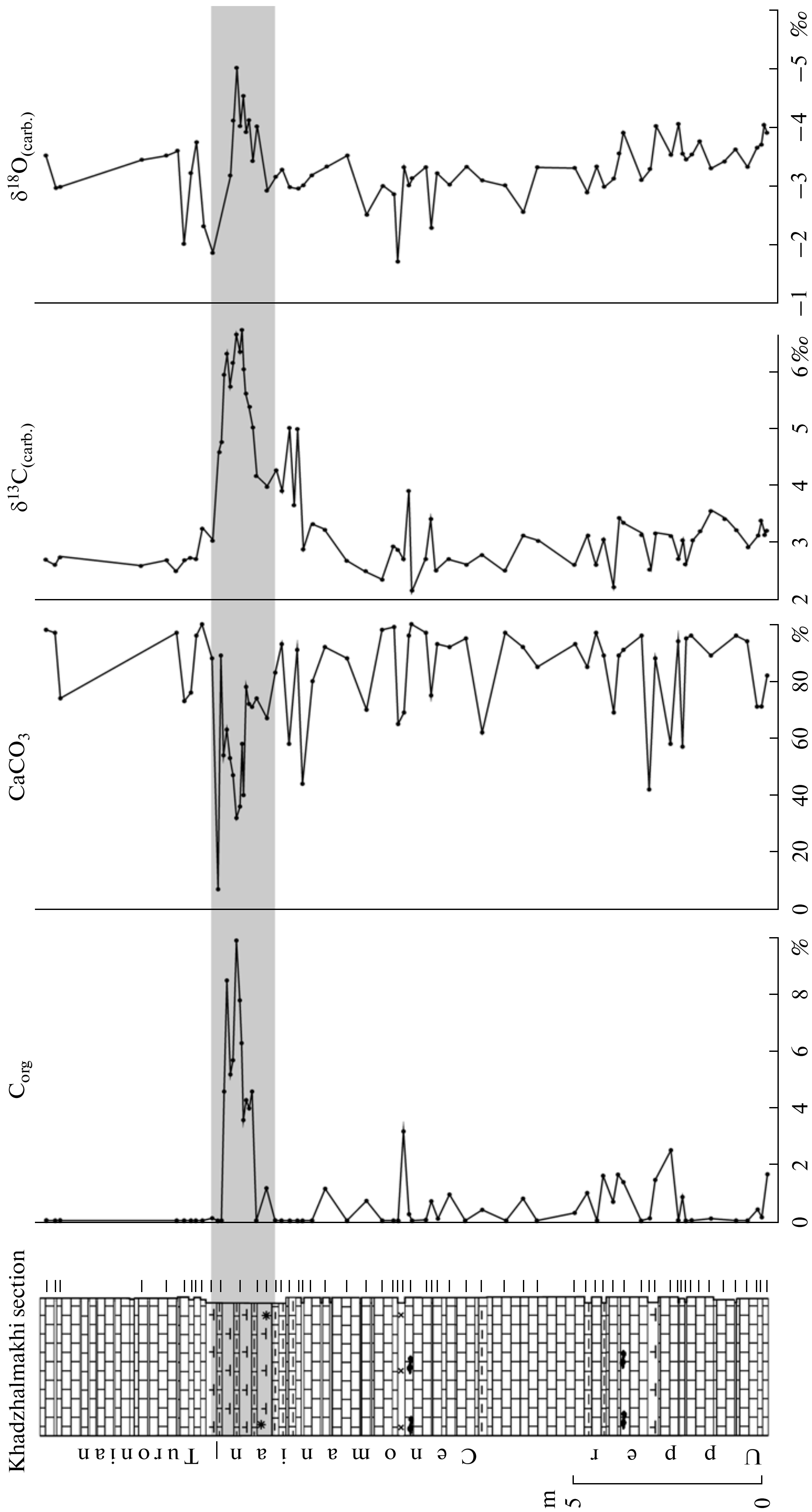

Fig. 13. Lithology of the transitional Cenomanian–Turonian sediments in the Khadzhalmakhi section and distribution of C_{org}, $CaCO_3$, $\delta^{13}C$, $\delta^{18}O$, and Ba.

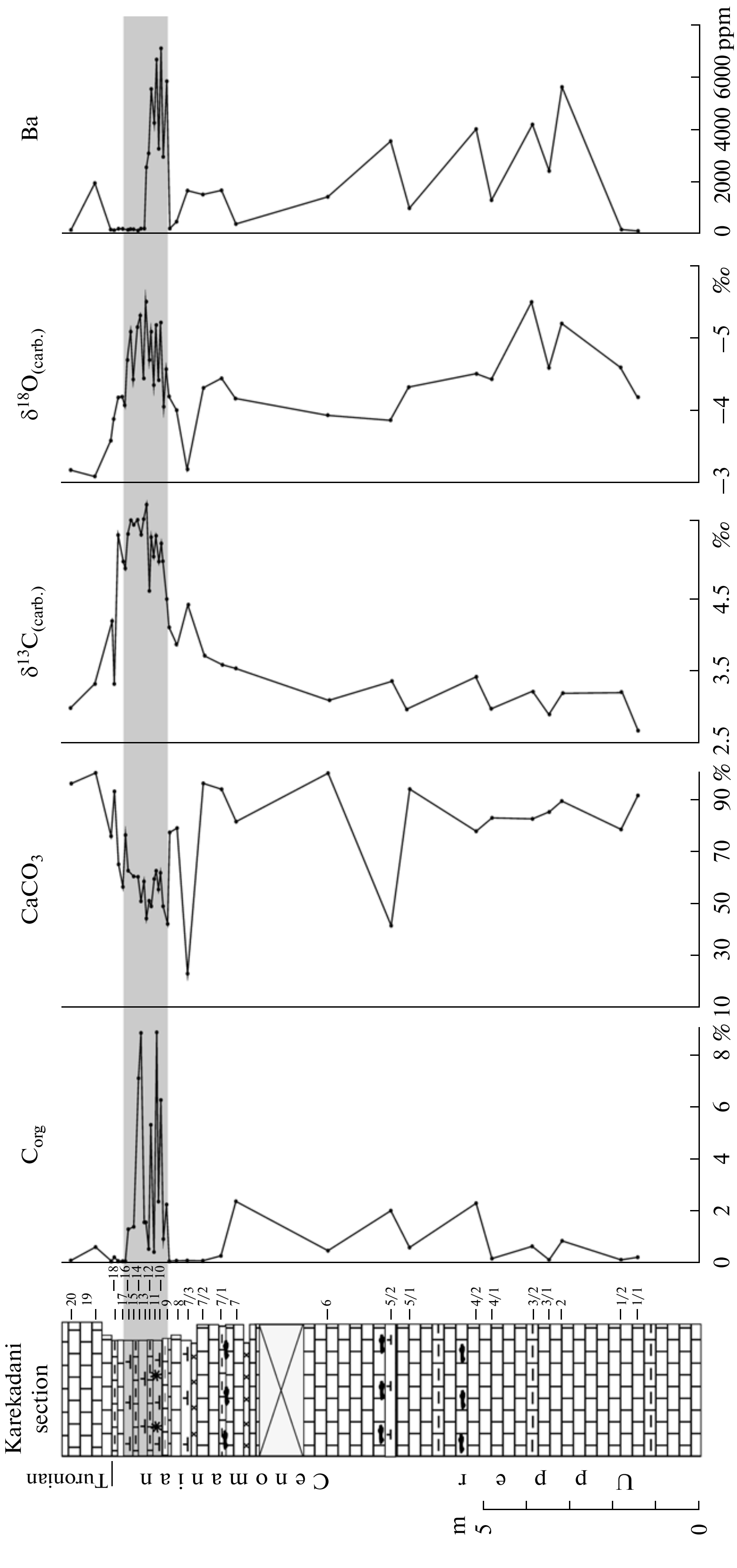

Fig. 14. Lithology of the transitional Cenomanian–Turonian sediments in the Karekadani section and distribution of C_{org}, $CaCO_3$, $\delta^{13}C$, $\delta^{18}O$, and Ba.

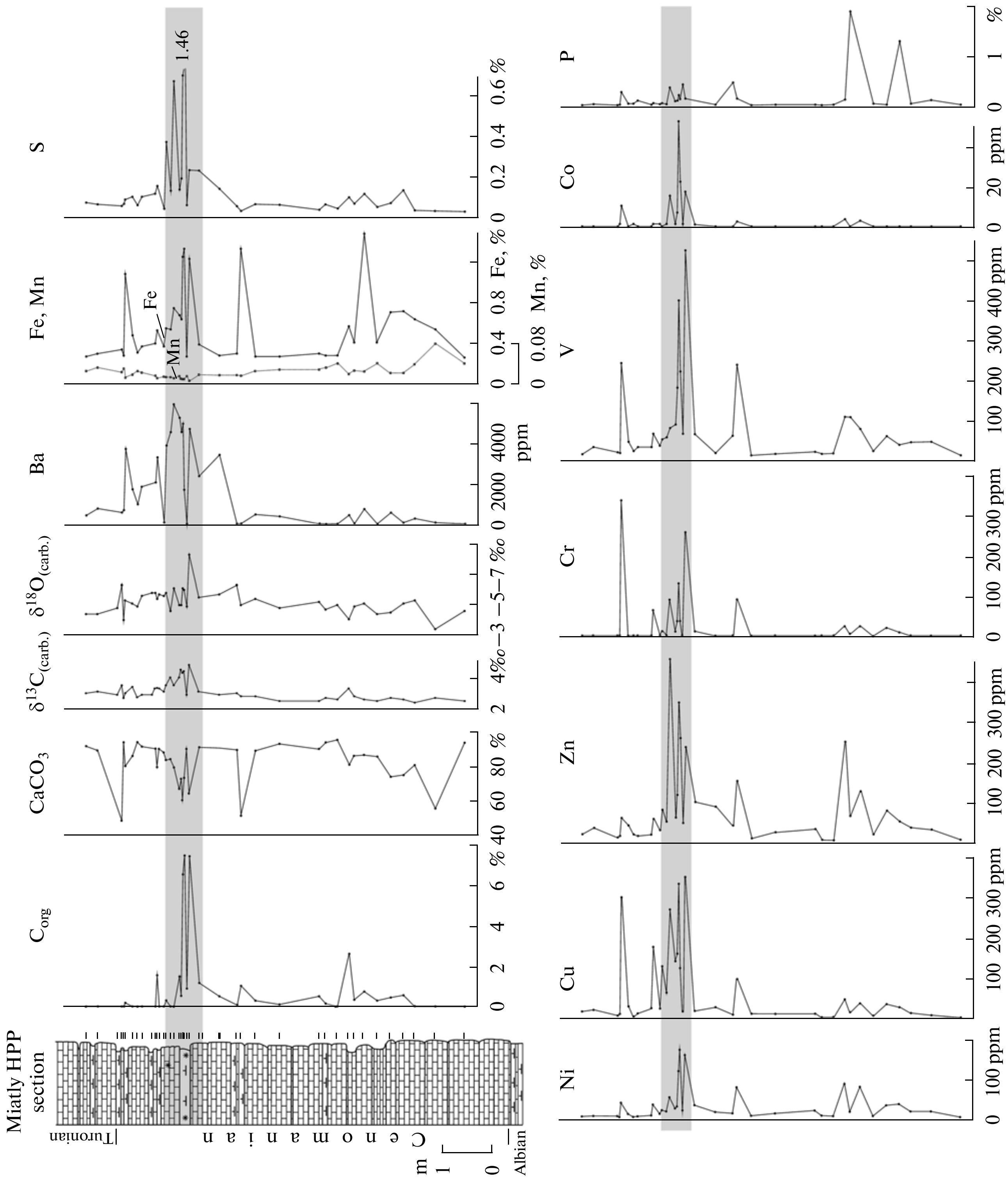

Fig. 15. Lithology of the transitional Cenomanian–Turonian sediments in the Miatly HPP section and distribution of C_{org}, $CaCO_3$, $\delta^{13}C$, $\delta^{18}O$, and some chemical elements.

samples 322–327). The structureless aggregates of OM are characterized by brown color with variable tints. The growth of C_{org} concentrations correlates with the increased sizes of colloalginite lumps.

In high-carbonaceous varieties, colloalginite lumps are large and abundant. The rocks also contain small-sized detritus of terrestrial organic matter as black or dark brown plant tissue fragments. In sedi-

Table 1. Results of the pyrolysis of organic matter

Member	Sample	T_{max}, °C	S1, mg HC/g rock	S2, mg HC/g rock	TOC, % of rock	HI mg HC/g TOC
Aimaki section						
II	331 b	435	0	0.13	0.014	92
	331	431	0.05	0.57	0.4	142
	330	429	0.18	8.8	2.54	346
γ	329	426	0.01	0.15	0.23	65
	328 e	434	0.03	1.31	0.74	177
	328 d	430	0.01	0.48	0.7	68
	328 c	431	0.03	2.98	1.68	177
	328 b	430	0.02	1.7	1.12	151
	328 a	430	0.1	0.89	0.48	185
β	327	415	0.32	53.9	7.76	694
	326	415	0.53	62.93	12.16	517
	325	422	1.26	35.43	7.08	500
	324-2	426	0.11	0.84	0.64	131
	324-1	412	0.57	40.41	7.66	527
	323	429	0.07	10.16	2.66	381
	322	415	0.23	41.36	7.63	542
	321	420	0.26	12.06	2.6	463
I	445	429	0.04	5.98	2.41	248
	443	429	0.03	0.39	0.3	130
Levashi section						
β	180-8	421	0.4	21.68	4.68	463
	180-7	432	0.08	1.24	0.63	196
	180-6	427	0.11	4.61	1.48	311
	180-5	431	0.05	1.58	0.64	246
	180-4	418	0.28	30.02	5.73	523
	180-3	420	0.76	81.53	8.26	446
	180-2	428	0.04	0.84	0.64	131
	180-1	413	0.53	43.69	7.96	548
I	07b	428	0.05	1.34	0.78	171
	06t	432	0.07	3.5	1.15	304
	05t	419	0.03	0.32	0.23	139
	04v	429	0.21	5.16	1.2	430

(I, II) Intervals of members under- and overlying the OAE 2 sediments; (β, γ) different members of the OAE 2 sediments; (T_{max}) temperature of the maximal extraction of hydrocarbon compounds during sample heating in the inert atmosphere (S1) bitumoid content in rock; (S2) petroleum potential of kerogen preserved in the analyzed sample; (TOC) total organic carbon content in rocks; (HI) hydrogen index.

ments under- and overlying the SB, organic matter occurs usually in the finely dispersed form. It is difficult to determine the nature of finely dispersed OM in carbonate rocks by petrographic methods. Admixture of plant detritus in the sediments under consideration is relatively low. Nevertheless, precisely such organic matter is dominant, since no remains of marine organisms are preserved in sediments.

Table 1 presents the results of pyrolytic analysis of OM in the Aimaki and Levashi sections[1]. They show that organic matter in the highly enriched in OM OAE 2 sediments differ from that in the host (upper Cenomanian) sequence. In sediments deposited prior to and after OAE 2, the hydrogen index (HI) value is usually <200 mg HC/g TOC (up to >340 mg HC/g TOC in some samples). Thus, kerogen in the host sequence belongs mostly to types II and III (Lopatin and Emets, 1987). In OM-rich sediments of OAE 2, the HI values increase up to 500–700 g HC/g TOC (kerogen of types I and II). At the same time, these rocks include intercalations with low C_{org} concentrations and moderate HI values, which decrease to 130 units (kerogen of type II). Such values imply that the sapropelic OM prevailed over terrestrial OM during the deposition of OM-rich sediments. However, the proportion between marine and terrestrial OM changed during a relatively brief period: the share of sapropelic OM decreased, while the terrestrial component substantially increased.

The study of the OM macerate extracted from the SB revealed that it is entirely represented by amorphous aggregates consisting likely of algal material and bacterial plankton. The SB is lacking in remains of organic-walled phytoplankton (G.N. Aleksandrova, pers. commun.). Taking into consideration the composition of OM in the highly enriched in OM sediments, it can be termed as sapropelitic OM.

As follows from the above-mentioned data, C_{org} and $CaCO_3$ in the upper Cenomanian sediments demonstrate opposite trends: growth in OM concentrations is accompanied by the decrease in carbonate contents. However, $CaCO_3$ remains the main rock-forming component even in the intervals marked by its lower content. Calcite is readily identified based on numerous diffractometric analysis data.

In all studied sections of Dagestan, the $CaCO_3$ content in limestones underlying the OAE 2 sediments varies from 85 to 90% and decreases to 50–60% in thin marlstone intercalations (Figs. 11–15). However, its share begins to decrease (although with some variations) in sediments underlying the SB. The OM-rich sediments are universally characterized by a progressive decrease of $CaCO_3$ concentrations. In the Aimaki section, the $CaCO_3$ content in the upper Cenomanian sediments overlying the SB slightly increases, although it never amounts to values characteristic of rocks older than the late Cenomanian event. In the section where the middle Turonian limestone onlaps the SB, the $CaCO_3$ content can rapidly increase up to >90%.

Chemical elements in OAE 2 sections

The geochemical properties of the OAE 2 sediments in different areas of the world are discussed in many publications, with consideration of the behavior of different chemical elements in them and mechanisms that influenced their concentrations in the OM-rich rocks (Arthur et al., 1988, 1990; Brumsack, 1980, 1986, 2006; Jarvis et al., 2001, 2008; Scopelliti et al., 2004; Snow and Duncan, 2005; Turgeon and Brumsack, 2006; and others).

In Dagestan, the behavior of a number of chemical elements was investigated in the OAE 2 OM-rich sediments as well as in the upper Cenomanian hosting rocks. These investigations included measurements of Al, Si, S, Fe, Mn, Ti, P, V, Cr, Ni, Co, Cu, Zn, Pb, As, Mo, Se, Ga, Ge, Ba, Sr, Rb, and some other elements. Some of them demonstrate a distinct trend of concentration in the OM-rich sediments, while others show slight or no response to the increase or decrease of OM in the OM-rich sediments (Table 2) (Gavrilov et al., 2009).

Most minor elements are characterized by the growth of their concentrations in OM-rich sediments, although the variations are very significant.

Barium is one of the elements characterized by appreciable variations of concentration in sediments associated with OAE 2. Its behavior in the Aimaki section is extremely remarkable. In sediments underlying the SB, its average content is approximately 400 ppm and varies from 70 to 1200 ppm (in one sample). Its concentration increases to 3700 in the lower part of SB and almost 6000 ppm (i.e., an order of magnitude higher, on the average), in the upper part. Noteworthy is the behavior of this element along the section: the C_{org} content significantly falls in sediments overlying the SB, while the Ba content is almost two times higher (~2500 ppm). Its content is reduced to the level preceding the SB accumulation (~350 ppm) only in the overlying member; i.e., the decrease is relatively gradual (Table 2, Fig. 11).

In general, a similar Ba behavior is observed in the OAE 2 sediments in the Levashi section. The difference consists only in relations between the SB and the overlying Turonian limestones: their boundary is distinctly erosional, which determined the sharp upper boundary of the Ba-rich interval.

In the Miatly HPP section, where boundaries of the OAE 2 sediments are vague, Ba is concentrated in a stratigraphic interval wider than that of marlstones highly enriched in OM (Figs. 7f, 15). Moreover, simi-

[1] The TOC (total organic carbon) and C_{org} concentrations in Tables 1 and 2, respectively, slightly differ from each other in absolute values (C_{org} concentrations are lower), although they demonstrate similar variation trends of organic matter in the section. These discrepancies show systemic patterns caused by differences in analytical methods (Ginsburg, 1991; *Metody* ..., 1957).

Table 2. Concentrations of chemical elements in the transitional Cenomanian/Turonian sediments of the Aimaki section

Member	Sample	C_{org}	$CaCO_3$	Fe	Mn	Ti	P	S	Ba	V	Ni	Cu	Zn	Pb	As	Se	Mo	Ga	Sr
II	335-2	0.19	82.32	0.71	0.013	0.132	0.05	<0.1	128	35.7	12	2.3	30.4	17.1	14	<0.5	1.4	3.4	489.9
	335-1	0.32	74.25	0.73	0.014	0.138	0.08	<0.1	250	36.7	12.6	31.9	39.6	8.4	9.5	<0.5	1.7	4.2	592.8
	334-2	0.26	76.84	0.59	0.033	0.067	0.05	<0.1	160	23	2.6	9.0	26	21	7	<0.5	1.5	5.1	730
	334-1	0.24	51.64	1.28	0.024	0.150	0.07	<0.1	250	52	14	35	68	14	<1	<0.5	<0.5	7.1	760
	333-1	<0.1	78.20	0.74	0.035	0.093	0.08	<0.1	170	33	4.9	18	34	20	9.1	<0.5	1.4	5.9	590
	332-3	<0.1	88.30	0.39	0.038	0.042	0.04	<0.1	160	10	<1	6.9	23	17	13	<0.5	2.1	5.7	630
	332-1	<0.1	79.00	0.60	0.016	0.066	0.04	<0.1	990	35	15	50	76	13	7.7	0.5	<0.5	5.4	980
	331 b	1.52	50.49	1.27	0.002	0.178	0.06	<0.1	1697	44	19.8	25	49	11	9	0.5	2.0	5	833
	331-2	0.14	77.41	0.67	0.021	0.076	0.05	<0.1	560	35	4.9	24	30	23	7.2	<0.5	0.7	5.2	810
	331-1	0.27	50.96	1.35	0.011	0.15	0.04	0.12	2700	76	27	89	72	11	9.0	0.6	1.2	7.9	750
	330-1	0.74	67.42	0.92	0.011	0.082	0.04	0.25	3200	64	28	110	72	13	14	2.1	2.6	6.3	880
γ	329-2	0.19	82.97	0.65	0.019	0.051	0.02	0.10	1200	33	12	39	46	23	14	0.5	2.0	5.1	960
	329-1	0.15	63.56	0.91	0.001	0.146	0.02	0.15	3594	40	23.7	52	67	15.8	10.8	2.1	2.5	3.7	849
	328 d-2	0.6	67.2	0.63	0.005	0.131	0.06	0.2	2955	36	14.2	29	41	7.3	8.1	0.9	1.3	1.7	887
	328 d-1	0.81	32.86	2.99	<0.001	0.331	0.08	0.24	4661	74	51.9	107	171	19.1	6.8	2.2	1.7	8.9	902
	328 c-2	0.2	83.11	0.68	0.003	0.123	0.02	0.1	2614	36	15.6	29	55	7.6	10.1	0.6	2	2	1031
	328 c-1	1.65	72.77	1.12	<0.001	0.127	0.1	0.3	4052	37	57	87	109	10.8	14.7	1.8	2.1	2.2	1106
	328 b-2	<0.1	68.45	0.41	0.001	0.122	0.05	0.14	1873	34	10.7	9	21	6.8	3.4	0.9	0.7	2.6	823
	328 b-1	0.46	67.08	1.05	0.001	0.149	0.08	0.12	3984	40	22	37	67	15	7.1	1	0.5	3.3	1004
	328	0.37	51.98	1.05	0.010	0.14	0.09	0.24	3190	81	15	56	62	19	3.0	0.7	<1	7.1	810
β	327-2	2.69	53.69	1.57	0.0085	0.13	0.08	0.45	4623	240	45	100	240	24	10	4.4	2.8	6.5	890
	327-1	7.30	46.88	2.91	0.0077	0.12	0.28	0.89	6408	410	120	70	190	17	17	5.6	12	5.1	1000
	326-2	8.30	58.34	1.61	0.0077	0.067	0.39	1.46	4987	150	83	47	200	22	15	5.4	8.1	4.5	1000
	326-1	6.00	45.17	1.36	0.0071	0.12	0.12	4.47	6730	210	69	130	250	14	11	5.0	1.9	6.5	840
	325	4.20	50.05	1.27	0.0093	0.11	0.11	0.74	7130	110	54	170	260	19	10	4.8	1.3	7.3	890
	324-2	0.68	59.25	1.06	0.011	0.099	0.18	0.29	3930	130	21	52	71	21	10	2.0	2.7	7.4	870
	324-1	3.40	62.31	1.83	0.010	0.079	0.23	1.30	6320	130	65	71	120	23	13	4.8	5.6	5.5	1000
	323	1.92	48.01	1.66	0.010	0.15	0.12	0.50	4530	130	35	78	140	18	<1	2.3	<1	7.1	770
	322	5.20	70.82	1.73	0.012	0.048	0.13	2.88	2180	74	68	34	70	25	14	1.9	6.4	4.1	960
	321á	3.55	81.38	1.47	0.017	0.025	0.1	0.46	1630	38	60	15	52	19	17	1.9	4.4	3.9	1100
α	321à	<0.1	71.73	0.71	0.020	0.070	0.05	0.12	170	51	9.1	20	39	16	9.1	<0.5	1.2	5.2	730
	320	<0.1	78.09	0.74	0.039	0.070	0.04	<0.1	117	27	10	11	22	14	6.9	<0.5	1.0	5.7	610
	336-1	<0.1	88.53	0.32	0.048	0.040	0.02	<0.1	72	4.0	1.2	5.5	12	19	8.0	<0.5	0.7	4.3	690
	336-2	<0.1	49.49	1.88	0.017	0.23	0.32	<0.1	1200	97	24	37	78	20	<1	<0.5	<0.5	9.5	710
I	337-1	<0.1	94.66	0.14	0.033	0.020	0.02	<0.1	180	7.8	1.5	3.9	15	21	13	<0.5	1.1	4.2	780
	338-1	0.24	91.71	0.16	0.029	0.020	0.02	<0.1	220	8.3	1.2	5.6	14	22	14	<0.5	1.9	4.6	780
	338-2	0.94	84.44	0.17	0.023	0.030	0.01	<0.1	270	7.8	3.4	7.5	17	22	14	<0.5	1.7	4.4	840
	339-1	<0.1	93.07	0.18	0.020	0.030	0.02	<0.1	340	12	2.8	8.2	7.0	23	12	<0.5	1.6	4.3	920
	339-2	0.47	87.74	0.39	0.016	0.040	0.04	0.22	980	32	16	34	64	23	12	<0.5	1.6	5.1	1000
	830-2	<0.1	93.23	0.1	0.03	0.02	0.04	0.06	223	14	6.4	5.7	16	<1.5	<1.5	<0.5	1.5	1.9	671
	830-1	<0.1	84.02	0.09	0.03	0.02	0.03	0.06	141	11	6.9	3.2	12	<1.5	<1.5	<0.5	1.2	2.5	646
	829	0.32	90.28	0.15	0.03	0.03	0.04	0.04	233	15	8.4	9.3	19	<1.5	<1.5	<0.5	1	2.5	700

(I, II) Intervals of members under- and overlying the OAE 2 sediments; (α, β, γ) different members of the OAE 2 sediments; contents of C_{org}, $CaCO_3$, Fe, Mn, Ti, P, and S are given in %; other elements, in ppm.

larly to the Aimaki section, the decrease in Ba concentrations (against the background of their fluctuations) is relatively gradual.

It is important that the Ba distribution along some OAE 2 sections is slightly different. For example, concentrations of this element in the SB of the Karekadani section are substantially variable: they range from 2500 to >7000 ppm in the lower part and sharply decrease at some levels within the black shales. In the upper part of the SB, the Ba concentration is 70–160 ppm, although the C_{org} content here is also high (7–9%). Noteworthy is also the fact that the C_{org} content at some levels in the limestone member underlying the OAE 2 sediments increases to 2.3%, while Ba concentrations in them amount to 3500–5500 ppm (Fig. 14).

No increase in the Ba content is observed in the OAE 2 sediments of the Khadzhalmakhi section, although the content increases gradually to 6500 ppm in OM-rich sediments of the same interval in the section located 5 km away. Such a behavior of Ba is most likely explained by its intense diagenetic redistribution in the OAE 2 sediments.

High Ba concentrations within the SB are characteristic not only for Dagestan OAE 2 sediments, but for other areas in the Crimean–Caucasus region. For example, high Ba contents (as high as 4100–6200 ppm) are detected in the OAE 2 carbonaceous sediments of Crimea (Aksudere section). At the same time, Ba concentrations in highly enriched in OM rocks (Corg up to 20%) of the Lazarevskoe section in the western Caucasus region are low (750–1450 ppm). High Ba concentrations were also noted in the Crimean OAE 2 sections in (Levitan et al., 2010).

Substantial increase of Ba concentrations in the OAE 2 sediments is likely a relatively stable trend. For example, in rocks from the coeval interval in the Umbria-Marche Basin of Italy, the Ba contents are as high as 1.4% (Turgeon and Brumsack, 200).

High positive correlation with the C_{org} distribution and elevated concentrations in OAE 2 OM-rich sediments are characteristic of several elements, such as V, Ni, Cu, Zn, Mo, Se, and S. The same, although considerably less expressed, trend is noted for Fe, P, Co, Cr, Rb, and Sr. The weakest response to changes in the sedimentation regime is demonstrated by Ti, Pb, Ga, and Ge.

As was mentioned, the $CaCO_3$ content in the OAE 2 sediments is lower than in the host sequence. The similar behavior is characteristic only of Mn: all the examined sections exhibit manifold decrease in its concentrations (Table 2, Figs. 15, 16). The similar trend is also observed in sections of the Northern Peri-Tethys within the intervals corresponding to other anoxic events: OAE 1a (Selly) and event at the Paleocene/Eocene boundary (PETM) (Gavrilov et al., 1997, 2002; Gavrilov, 2003).

The general trend of growth or reduction of element concentrations in the OAE 2 sections is complicated by their distinct cyclic patterns owing to variations in C_{org} and $CaCO_3$ concentrations. Correspondingly, the distribution of elements is also irregular, which is well seen in the Khadzhalmakhi section (Fig. 16). In lower C_{org}-rich parts of cyclites, concentrations of elements are usually maximal, while their upper parts exhibit sharply reduced contents of many elements. Nevertheless, absolute values of element concentrations remain notably higher than in sediments that underlie and overlie the OAE 2. Other Dagestan sections demonstrate generally similar patterns in the distribution of chemical elements in the upper Cenomanian sequence (Table 2, Fig. 15). Thus, these elements are characterized by the stable positive correlation with C_{org} concentrations. At the same time, maximal C_{org} concentrations in rocks are not always (to be more exact, rarely) correlated with maximal contents of elements; i.e., no positive quantitative correlation exists between these parameters.

The complex nonlinear distribution of chemical elements is observed both inside particular OAE 2 sections and over the areal extent of these sediments.

In the eastern Caucasus basin, concentrations of chemical elements in the OAE 2 are also variable. For example, comparison between their maximal concentrations in OM-rich layers in different sections revealed that their values are highly variable (in ppm): Zn 260–670, Ni 120–230, Cu 170–350, Co 16–53, Cr 75–260, V 240–520, As 15–36, Mo 12–45, Se 5.6–17.7. Noteworthy is the universal substantial increase of sulfur concentrations in OAE 2 sediments up to >1.5% or even several percents in singles samples (up to 4.5% in the Aimaki section, Table 2).

Carbon and oxygen isotopes in the upper Cenomanian sediments

Similar to most areas of the world (Schlanger et al., 1987; Tsikos et al., 2004; and others), the OAE 2 sediments exhibit positive $\delta^{13}C$ and negative $\delta^{18}O$ anomalies, relative to host sediments of Dagestan sections. As follows from Fig. 11, changes in the $\delta^{13}C$ and $\delta^{18}O$ values in the stratigraphically most complete Aimaki section are relatively regular. In sediments underlying the SB, the $\delta^{13}C$ value varies from 2.7 to ~3.5‰. The trend $\delta^{13}C$ growth trend is already notable immediately below the SB. Transition to sapropelic sediments is accompanied by the growth of $\delta^{13}C$ up to >5‰. At the same time, these values within the SB are variable: maximal $\delta^{13}C$ values are observable in the lower (5.1–5.2‰) and upper (5–5.6‰) parts of the SB, while the middle part exhibits relative decrease to 4.4–4.8‰. Above the SB, $\delta^{13}C$ gradually decreases down to minimal values in the basal part of the Turonian sequence.

A similar behavior of $\delta^{13}C$ is also observed in other sections of the eastern Caucasus (Figs. 14–17). They demonstrate the growth of $\delta^{13}C$ already in marlstones

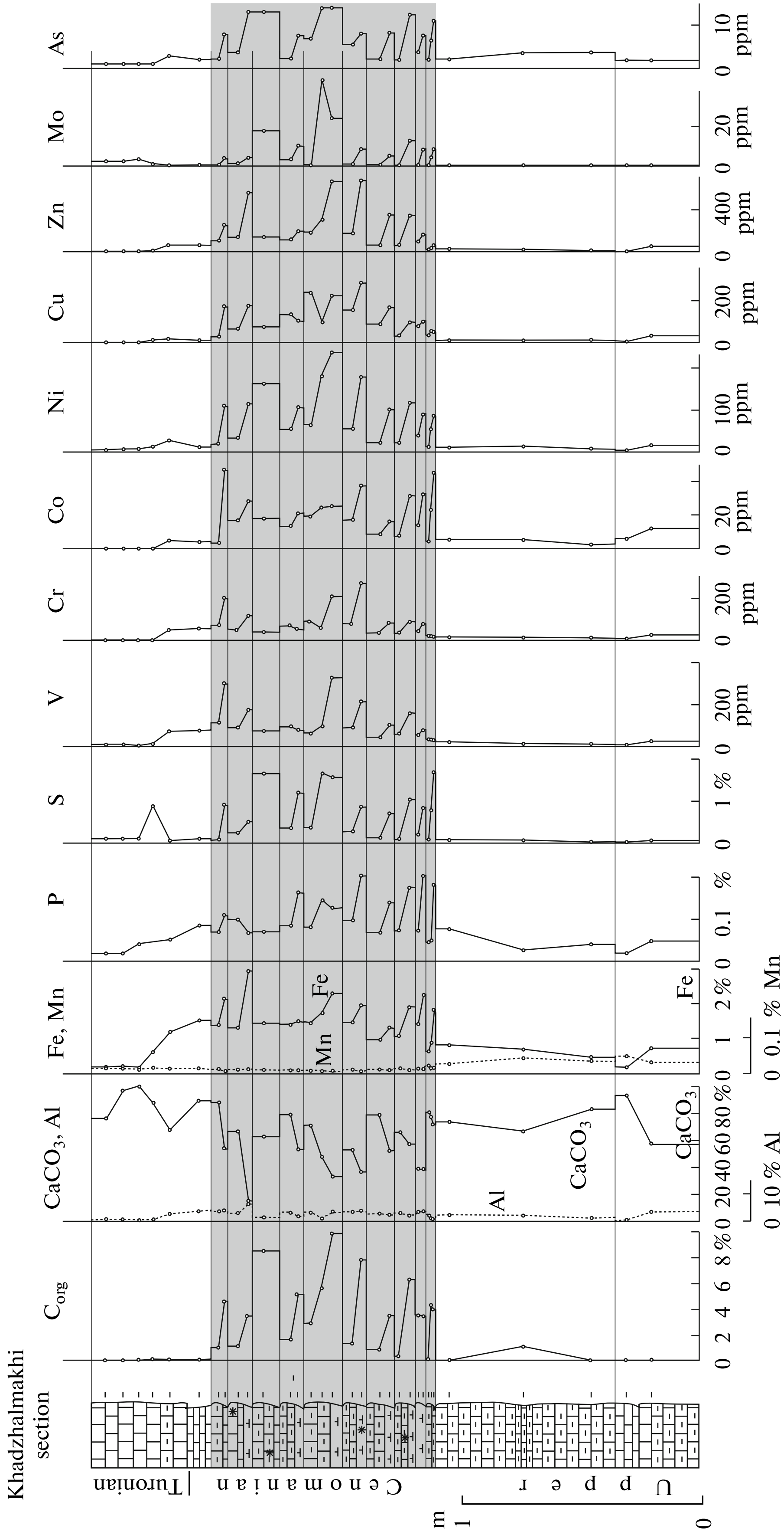

Fig. 16. Distribution of chemical elements in cyclites of the carbonaceous member in the Khadzhalmakhi section.

underlying the SB (Layer α). Variations in the $\delta^{13}C$ values in this horizon are low and never exceed 1‰. In addition, they are irregular. The absolute $\delta^{13}C$ values are also similar in different sections. Only in the Miatly section, the carbon anomaly is relatively low and never exceeds 4.8‰. It should be noted that similarly to the Aimaki section, the upper boundary of the isotope anomaly in the section under consideration is characterized by gradual decrease in the $\delta^{13}C$ value.

The $\delta^{18}O$ values also regularly change in OAE 2 sediments. In the Aimaki section, the sequence underlying the SB includes two intervals: $\delta^{18}O$ values range from –3.5 to –5‰ in the upper part of the limestone member and from –2.6 to –3.8‰ in the Layer α; i.e., the $\delta^{18}O$ values in this section exhibit a slight decrease. Two high negative $\delta^{18}O$ peaks separated by an interval with elevated values are observable at the base of the SB and its upper part. As shown in Fig. 11, low $\delta^{18}O$ values (with some variations) above the SB are characteristic of the uppermost Cenomanian layers only at the boundary with the Turonian sequence. The value increases substantially (up to –3‰) in the basal layers. Thus, the lower boundary of both isotope anomalies in the Aimaki section is rather sharp, while restoration of pre-crisis values is very gradual. In other examined sections, where the Turonian limestones rest upon the OAE 2 sediments with an erosional surface (Levashi, Karekadani, and Khadzhalmakhi), the upper boundary of the $\delta^{13}C$ and $\delta^{18}O$ anomalies is marked by sharp changes in their values and restoration of their background parameters that existed prior to the OAE 2 event (Figs. 12–14).

Within the SB, the $\delta^{13}C$ values demonstrate no stable correlation with C_{org} and $CaCO_3$ concentrations, in contrast to $\delta^{18}O$ values that exhibit such a correlation. In sections with distinct cyclic patterns, the increase of C_{org} concentrations (by several percents) in rocks is frequently accompanied by a slight decrease in $\delta^{18}O$ values, i.e., by the negative shift with the amplitude amounting to 1‰. It is conceivable that such a behavior of $\delta^{18}O$ values is determined by the influence of diagenetic processes.

TAXONOMIC CHANGES IN NANNOFOSSIL ASSEMBLAGES AND RECONSTRUCTION OF PALEOECOLOGICAL SETTINGS

Changes in proportions of different paleoecological nannoplankton groups reflect variations in environmental parameters (temperature, salinity, trophic regime). Therefore, the quantitative assessment of such changes represents one of the most important tools used in paleoecological reconstructions. It should, however, be kept in mind that the composition of nannofossil assemblages are affected by diagenetic alteration of sediments, in addition to ecological factors: dissolution and/or recrystallization can considerably modify the initial proportions between nannofossil taxa. Inasmuch as nannofossil assemblages from the transitional Cenomanian–Turonian interval of the Aimaki section are generally impoverished, we estimated only proportions of their most abundant taxa, including *Watznaueria* spp. (most resistant to environmental changes and diagenetic transformations), warm-water *Rhagodiscus* spp, (*R. asper, R. achlyostaurion, R. sageri*, and others), and cool-water *Eprolithus* spp. (*E. floralis, E. apertior, E. octopetalus, E. eptapetalus*). *Eiffelithus* spp. (*Eifellites turriseiffeli* and related species (Shamrock and Watkins, 2009) included), *Quadrum intermedium*, and *Zeugrhabdotus embergeri*, which likely represent taxa resistant to diagenetic transformations. For estimating proportions between different groups, 300 randomly selected specimens were counted. No counting was performed for nannofossil assemblages from the lower part of the interval under consideration, since their abundances were insufficient for reliable statistics.

As compared with the lower–middle Cenomanian nannofossil assemblages from the Dagestan sections, the upper Cenomanian assemblages are characterized by low abundances, low species diversity, and poor preservation, which is likely explained by intense diagenetic transformations of rocks from this interval. In the Levashi and Karekadani sections, nannofossils are practically missing from the SB, which likely implies extremely unfavorable environments for the nannoflora in the basin at that time. The Aimaki section demonstrates most notable reorganizations in the composition of nannofossil assemblages. Compact limestones underlying the SB are depleted in nannofossils due to intense recrystallization of rocks. They contain only taxa resistant to diagenetic transformations: *Watznaueria barnesiae*, rare *Zeugrhabdotus embergeri, Tranolithus orionatus*, few *Rhagodiscus* spp., *Retecapsa* spp., and *Eprolithus floralis*. Sediments of the SB are characterized by slightly greater abundance and diversity of nannofossils as compared with host rocks. This situation can be explained by a less intense diagenetic recrystallization and relatively low dissolution of calcium carbonate. In addition, the sea level rise and the formation of marine settings substantially more favorable for the nannoflora development (relative to the shallow-water environments characteristic of limestones underlying the SB) could stimulate the nannoplakton abundance and diversity.

As a whole, the nannofossil assemblages from both SB and host rocks are dominated by *Watznaueria barnesiae* (Fig. 10), which is highly resistant to paleoecological changes and diagenetic transformations. This species was globally distributed during the Cretaceous. It is always difficult to discriminate the particular factor that stimulated mass occurrence of this species in different settings. Nevertheless, it seems that such a dominant role in the SB of the Aimaki section reflects primary high productivity owing to its distribution in ecological niches unfavorable for other nannofloral taxa. In addition, the nannofossil assemblage from the SB and overlying sediments corresponding to the late stage of the carbon isotope excursion includes rare eutrophic forms *Biscutum constans* and small *Zeugrhabdotus* spp., which constitute 1–3% in the SB and are missing from the underlying strata. Decrease of their abundance in the OAE 2 sediments was established in many paleobasins (Gale et al., 2000; Paul et al., 1999; Waslworth-Bell et al., 2003) and interpreted as indicator of the deficiency nutrients. In contrast, productivity of these species in other areas of the world increases considerably (El Sabbagh et al., 2011; Hardas and Mutterlose, 2007; Melinte-Dobrinescu and Bojar, 2008) reflecting development of more eurtophic settings. Abundance of some other dissolution-resistant taxa varies notably, although changes in the composition of the nannofossil assemblage within the SB cannot be considered as catastrophic.

The pre-crisis period encompasses a remarkable brief episode of relative warming marked by the elevated content of warm-water *Rhagodiscus* spp. and insignificant decrease in $\delta^{18}O$ values (Sample 337). The first indications of paleoecological changes are recorded in a gray marlstone layer (Layer α) underlying the SB. These rocks demonstrate slight increase in the share of cool-water genera *Eprolithus* and *Quadrum* against the background of notably reduced abundance of warm-water *Rhagodiscus* spp. and appearance of large *Assipetra terebrodentarius*, a typical Boreal form missing in Lower Cretaceous sediments which likely characterizes a brief cooling episode. In the upper part of Layer α, the situation changes: abundance of warm-water taxa rapidly grows (up to 20%), while cool-water forms temporally disappear from the assemblage. Despite significant variations in $\delta^{18}O$ values within the SB reflected in maximal negative shift in the upper part of the oxygen isotope curve, nannofossil assemblage exhibit a stable decrease of warm-water *Rhagodiscus* spp. and increase of *Eprolithus* and *Quadrum* representaives. Moreover, all coccoliths become extremely small, indicating environments unfavorable for the nannoflora (Tremolada et al., 2006; Weissert and Erba, 2004; and others). In many regions, increase of cool-water *Eprolithus* in the interval corresponding to OAE 2 is revealed (Erba, 2004; Melinte-Dobrinescu and Bojar, 2008; Waslworth-Bell et al., 2003) and frequently accompanied by the positive oxygen isotope shift, which is attributed to a brief cooling episode during OAE 2 (Jarvis et al., 2011). The notable decrease in temperature during this critical event is also confirmed by the TEX_{86} analysis (Sinninghe Damste et al., 2010). At the same time, the SB in Dagestan demonstrates relatively rapid decrease in $\delta^{18}O$ values (in general, by more than 2.5‰ in the Aimalki and Karekadani sections and by ~4.8‰ in the Levashi section), which could be related to significant warming and/or desalination of the basin. Nevertheless, the composition of nannofossil assemblages from the SB of the Aimaki section provides no grounds for either of these assumptions, because they are characterized by a relatively high diversity (>25 species) despite insignificant total abundance, in addition to the occurrence of cool-water taxa. This situation is unlikely even under insignificant salinity decrease. It might be assumed that such a nannofossil assemblage in the Levashi and Karekadani sections reflects freshwater ingression, since their nannofossil assemblages are extremely impoverished. However, the $\delta^{18}O$ values are substantially different in these sections and the values in the Karekadani section are close to those in the Aimaki section. Thus, the composition of nannofossil assemblages in the SB and oxygen isotope data are slightly contradicting, although the abundance of warm-water taxa is in a good agreement with $\delta^{18}O$ fluctuations below and above the SB.

After cessation of the deposition of OM-rich sediments, the pre-crisis proportions of nannoflora taxa became restored to the parameters characteristic of the terminal stage of the carbon isotope shift (Sample 329). This fact probably indicates that restoration of paleoecological conditions was gradual and environments relatively unfavorable for the nannoflora were retained during a long period after the disappearance of most critical settings.

Previous investigations of macrofaunal remains of the Upper Cretaceous sections of Dagestan were organized by F.G. Sharafutdinov in cooperation with M.M. Moskvin (Echinoidea), M.A. Pergament (Inoceramidae), Yu.P. Smirnov (Ammonoidea), and others. Analysis of the macrofauna distribution along the section revealed that abundance of ammonites and echinoids significantly decreases up to their disappearance near the OAE 2 level in the upper part of the Cenomanian sequence. This fact can also indicate deterioration of paleoecological conditions at that time.

DISCUSSION

For reconstructing the scenario of OAE 2 development in the eastern Caucasus basin, we should estimate its duration and define the corresponding sedimentary section. However, unequivocal solution of this issue is not an easy task. It is undoubted that the OM-rich sediments should be attributed to this event. At the same time, the C_{org} content in sediments is a very important (but not sole) parameter that characterizes this event: the behavior of carbon and oxygen isotopes, biotic changes, and distribution of some chemical elements should be taken into consideration.

Primarily, the level of the OAE 2 onset or, more exactly, first lithological, geochemical, and biotic signs of its manifestation in the Cenomanian sedimentary sections of Dagestan should be defined. It was mentioned above that the top of compact limestones overlain by marlstones and clayey limestones of Layer α corresponds to the distinct lithological boundary. Precisely this level is marked by first indications of paleoecological changes: increase in abundance of cool-water nannofossil genera against the background of drastic reduction of warm-water forms that dominated previously in the eastern Caucasus basin; notable decrease in the $CaCO_3$ content in sediments of Layer α as compared with the underlying limestone sequence (Figs. 11–15); and distinct trend of $\delta^{13}C$ growth. These features provide grounds for including the Layer α into the sedimentary sequence corresponding to OAE 2. These sediments were deposited in relatively shallow-water settings, where sedimentary material was subjected to reworking. As was mentioned, two (complete and incomplete) cyclites are definable in this layer in the most complete Aimaki section despite the poorly preserved sedimentary bedding patterns.

The layer of OM-rich sediment (β) is the most typical reflection of the Bonarelli Event and, probably, most drastic paleoecological changes. As follows from sections with the distinct cyclicity, they comprise up to 11 or 12 cyclites. The same number of sedimentary cycles (11) is cited in (Kuhnt et al., 2005). If the formation period of each cyclite is correlated with duration of the short-term Milankovitch precession cycles (~21 ka), duration of the deposition of OM-rich sediments can be estimated at 230–250 ka.

The Aimaki section also reflects changes in the geochemical and biotic parameters at the terminal stage of OAE 2 after the deposition of OM-rich sediments. As follows from Fig. 11, restoration of the $\delta^{13}C$ and $\delta^{18}O$ values up to the pre-crisis level was relatively gradual in sediments overlying the SB. Moreover, the carbon isotope anomaly terminated earlier than the oxygen anomaly. The most distinct carbon anomaly is traceable up to the top of Layer γ (Sample 329), which is also marked by restoration of the pre-crisis proportions between nannofossil taxa. Precisely this level should likely be considered as the level corresponding to OAE 2 termination at the present-day investigation stage.

Proceeding from the cyclic patterns of Layer γ, duration of its deposition can be estimated at ~105–125 ka. As for the poorly structured Layer α in the Aimaki section, its formation period was likely 30–35 ka long. In this case, the total duration of the OAE 2 in the eastern Caucasus sections based on the analysis of sedimentological, geochemical, and biotic data is estimated at approximately 370–410 ka. If the entire sedimentary cycle (members α, β, γ) including carbonaceous sediments (β) is correlated with the long eccentricity cycle, its duration is estimated at approximately 400 ka. This estimate is generally close to the values obtained from the correlation with precession cycles.

The available estimates of Bonarelli Event duration in other regions of the world are highly variable (in ka): 500–800 (Arthur et al., 1988); 240 (Kuhnt et al., 1997); 720 (Sageman et al., 1997]; 400 (Caron et al., 1999); 320 (Prokoph et al., 2001); 440 (Kuhnt et al., 2005); 563–601 and even 847–885 (Sageman et al., 2006). At the same time, duration of the positive carbon anomaly in the Pueblo section (Colorado) is estimated at 100 ka (Keller et al., 2004). The significant scatter in estimates of OAE 2 duration is likely explained by various factors: different degrees of the completeness of sedimentary sections, uncertainty in the position of its upper boundary, differences in assessment methods, and others.

The late Cenomanian Oceanic Anoxic Event (OAE 2) influenced the behavior of many chemical elements in the sedimentary process (Figs. 11–16, Table 2). However, increase in the concentration of most elements is primarily determined by the enrichment of sediments with organic matter. Beyond the SM, their contents usually correspond to background values. Only Ba deviates from this regularity: its concentrations are extremely high (more than an order of magnitude higher) both in and beyond the SB (Figs. 11, 12, 14, 15), suggesting that its behavior differs from that of the main group of examined chemical elements.

The intense investigation of the Ba behavior in the sedimentary process started after works by (Goldberg and Arrhenius, 1958), who assumed its potential significance for the assessment of bioproductivity based on the study of equatorial pelagic sediments. This assumption was repeatedly confirmed by subsequent researchers, who investigated Recent and Quaternary sediments along with some older rocks (Dymond et al., 1992; Falkner et al., 1993; Kasten et al., 2001; McManus et al., 1998; Paytan and Griffith, 2007; Pfeifer et al., 2001; Schmitz, 1987; von Breymann et al., 1992; and others). Dymond et al. (1992) showed distinct correlation between Ba and C_{org} in sediments. At the same time, some researchers note the absence of any correlation between these parameters (Kasten et al., 2001), which is explained by oxidation of organic matter in sediments accompanied by the decrease in C_{org} concentrations against the background of relatively high Ba contents. This phenomenon was most likely characteristic of the Cenomanian section in Dagestan. For example, sediments overlying the SB in the Aimaki section were initially characterized by high C_{org} concentrations. They decreased subsequently due to the oxidation of organic matter, while Ba concentration remained unchanged. Moreover, the oxygen influx to the more clayey and less porous sediments of the SB was hampered and the C_{org} content was not subjected to notable changes.

Of particular interest are the data on the Ba behavior in anoxic environments (Arndt et al., 2006; Falkner et al., 1993; Henkel et al., 2012; and others). In our opinion, the above-mentioned unusual Ba behavior (partial or complete absence of its elevated concentrations in OAE 2 carbonaceous sediments) in the Karekadani and Khadzhalmakhi sections is related to redistribution at the diagenetic stage. It was previously established that reducing environments in sediments stimulate the remobilization of Ba its migration, and concentration at some levels, i.e., the formation of the so-called “barium front” (McManus et al., 1998; Torres et al., 1996; and others). This process could promote the substantial decrease of Ba concentrations in rich in OM sediments. In the Dagestan OAE 2 sections, diagenetic redistribution of Ba could involve both the entire SB and its upper half. In the first case, concentrations of this element were low throughout the layer (Khadzhalmakhi section). In the second case, Ba concentrations remained high in the lower part of the sequence (Karekadani section). It is difficult at the moment to speak about factors governing the Ba behavior in sediments at the diagenetic stage. We believe that the unusual Ba distribution in these sections can be explained by the early Turonian erosion of sediments overlying the OAE 2 and resumption of the contact between OM-rich sediments, where diagenetic processes were in progress, and bottom water at that time.

Many researchers traditionally consider OAE 2 as one of the most remarkable global events marked by the development of anoxic environments in the bottom water layer of seas and oceans (Arthur et al., 1987; Jenkins, 1980; Schlanger et al., 1987; and others). Our data provide no grounds for an assumption of long-term stable anoxic environments in the late Cenomanian eastern Caucasus basin. We can definitely assume the existence of distinct reducing conditions in the OM-rich sediments, since they contain relatively abundant sulfide concretions and exhibit lamination (although not at all levels of the SB). Decrease or disappearance of the benthic fauna (foraminifers and others) and occurrence of fucoids left mainly by *Chondrites*, which could survive anoxia, indicate the oxygen deficiency in the bottom water layer. Inasmuch as sedimentation was a cyclic process, when the accumulation of OM-rich sediments alternated with the deposition of carbonate facies with relatively low C_{org} concentrations, geochemical conditions in both sediments and bottom waters changed from the anoxic to suboxic to, probably, normal oxic type. When reconstructing depositional environments in the late Cenomanian basin, we should take into consideration geochemical data on OAE 2 sediments in Dagestan sections, such as low Mo and Se concentrations (up to 40 and 15 ppm, respectively, in different sections). At the same time, these and some other redox-sensitive elements are usually concentrated in sediments of the H_2S-contaminated basins, where their contents much higher. For example, Mo and Se concentrations in the highly rich in OM sediments deposited in the Paleocene/Eocene basin (PETM Event) with anoxic environments in the bottom water layer are as high as 300–400 ppm (>1700 ppm in some samples) and 80–280 ppm, respectively (Gavrilov et al., 1997, 2003; Gavrilov and Shcherbinina, 2004). In sediments deposited in the Aptian anoxic basin of the East European Platform (Selly Event), Mo concentrations amount to 130 ppm (Gavrilov et al., 2002).

It should be kept in mind that the Late Cenomanian sea was relatively shallow, and this factor should restrict the development of anoxia. Therefore, in our opinion, development of anoxic environments in the bottom water layer should lead to the following consequences: first, they should involve a relatively small part of the water column; second, the degree of oxygen deficiency in the water should vary substantially during the accumulation of the SB owing to the cyclic sedimentation pattern; and finally, anoxia should weaken during the intensification of hydrodynamic activity due to the relatively shallow depth of the basin.

It should be noted that the absence of anoxic environments in some late Cenomanian basins during the OAE 2 is suggested in (Westermann et al., 2008).

Problem of the presence or absence of anoxic environments in the late Cenomanian basin is closely related the issue of origin and formation mechanisms of the OM-rich sediments. Inasmuch as no stable anoxia existed in the late Cenomanian eastern Caucasus basin, this property could not serve as a main factor responsible for the deposition of OM-rich sediments. Another factor, which could be responsible for this phenomenon, was the intense growth in productivity of the organic-walled phytoplankton and bacterial plankton.

Correspondingly, the question arises as to what factor triggered the productivity outburst primarily during periods of the intense influx of biophile elements into the basin. Upwelling is a well-known process that stimulates the high supply of biophile elements to zones of the high present-day productivity. However, its efficiency is very low in shallow and spacious epicontinental seas.

The formation of the SB during the OAE 2 Event is most satisfactorily explained by the input of biophile elements from the coastal onshore landscapes in response to rapid eustatic transgressions. This model was based on the analysis of formation conditions of the lower Toarcian organic-rich sediments in the northern Caucasus basin, Aptian sediments in the Russian Plate (OAE 1a), and Paleocene/Eocene anoxic event (PETM) in the northeastern Peri-Tethys (Gavrilov, 1994; Gavrilov and Kopaevich, 1996; Gavrilov et al., 1997, 2002, 2003; Gavrilov and Shcherbinina, 2004). It was established that the following settings were favorable for accumulation of organic matter in sediments.

During the regressive episodes before transgressions, the exposed spacious areas of the sea bottom along coasts and around archipelagos covered by poorly consolidated sediments were readily subjected to erosion, particularly when they contained a notable share of diagenetic sulfides. These areas were occupied by lacustrine–boggy landscapes with rapid accumulation of OM (both in solid (plants) and dissolved phases). The acid medium of peatlands stimulated the transfer of many elements (including biophile varieties) into solution. Thus, regression stimulated the development of specific geochemically active coastal landscapes, which accumulated reactive substances (organic matter; compounds of P, N, Fe, and other elements).

Subsequently, the regression gave way to the rapidly developing transgression and the advancing landward sea interacted with these landscapes. Consequently, significant quantities of biophile elements, as well as dissolved and solid terrestrial OM, were transported to the basin. The intense transport of terrestrial OM from land is evident from the pyrolytic analysis of samples from the OAE 2 sediments. Involvement of biophile elements in the biological cycle stimulated an intense bloom of phyto- and bacterioplankton, resulting in the enrichment of sediments with OM and the intermittent development of anoxic environments in the bottom water layer. Moreover, in the case of poorly differentiated relief of the peneplained seafloor, even insignificant sea level rise provoked the flooding of spacious areas and the mobilization of significant quantities of biophile elements. Input of these elements stimulated a sharp growth of productivity in the basin.

Transgression was relatively rapid but irregular, as suggested by cyclic patterns of the SB (over 10 cyclites). Probably, the intermittent transgression retarded or even stopped because of short-period sea level fluctuations related to the Milankovitch precession cycles. Such irregular development and discreteness of the transgression resulted in the decreased influx of biophile elements to the basin, lower productivity of phyto- and bacterioplankton, and accumulation of OM-depleted sediments (mostly calcareous). The influx of biophile elements to the basin depended to a significant extent on local geomorphological properties of coastal landscapes. Vast flat or gently inclined landscapes were most favorable for the influx of biophile elements, while the relatively steep coasts caused accumulation of sediments with low C_{org} concentrations.

Termination of the most active phase in the transgression and, correspondingly, cessation of the delivery of biophile elements to the basin were followed by the gradual fall of phytoplankton bloom and reduction of OM accumulation in sediments.

This mechanism of the formation of OM-rich sediments satisfactorily explains the origin of their relatively thin sequences (similar to those in OAE 2) that are spread over a spacious territory.

Thus, eustatic sea level fluctuations of different signs, orders, and amplitudes are crucial in the formation of OM-rich sediments. Different aspects of sea level fluctuations in the terminal Cenomanian are discussed in (Gale et al., 1999, 2002; Robaszynski et al., 1998; Voigt et al., 2006; Wilmsen, 2003).

Many publications are dedicated to changes in different marine ecosystems during the OAE 2 episode. This event was accompanied by changes in the gas composition of the atmosphere, which is evident from the carbon anomaly in terrestrial plant remains (Hasegava, 1997). Despite the criticism in (Yazykova and Zonova, 2004) addressed to some reconstructions proposed by Hasegava (1997), his general concepts seem to be quite correct. Thus, changes of paleoecological environments in the late Cenomanian were characteristic of oceanic and marine systems, atmosphere, and terrestrial landscapes. It means that some changes were typical of the whole biosphere. Therefore, the OAE 2 phenomenon can be classed as the biospheric event.

CONCLUSIONS

(1) The late Cenomanian Oceanic Anoxic Event (OAE 2) is readily recognizable in the sedimentary record of the eastern Caucasus basin, which represented a constituent of the northeastern Peri-Tethys. Sediments of the transitional Cenomanian/Turonian interval were investigated in seven sections. Based on the stratigraphic completeness, the sections are dived into three types: (1) sections with complete OAE 2 interval; (2) sections containing only the OM-rich sediments overlain by the middle Turonian limestones; and (3) sections marked by the complete erosion of OAE 2 sediments during the early Turonian transgression.

(2) The OAE 2 sediments are characterized by a distinct cyclic structure. The SB comprises 11 or 12 cyclites each up to 15–17 cm thick. The cyclites consist of alternating black marlstones (at the base) and gray clayey limestones. The sediments rich in OM (Layer β) together with the under- and overlying sequences (layers α and γ) form a single sedimentary cycle.

(3) OM-rich sediments differ from their host rocks by the litho geochemical, and paleontological properties: they demonstrate positive $\delta^{13}C$ and negative $\delta^{18}O$ anomalies, elevated concentrations of many minor elements, substantial reorganizations in nannofossil assemblages, disappearance of benthic organisms, and others. Since some changes are observable already in the underlying Layer α and traced up to the top of Layer γ, the whole assemblage of sediments of this interval can be assigned to the OAE 2.

(4) Analysis of changes in the nannofossil assemblage composition in the transitional Cenomanian–Turonian interval revealed indicators of drastic environmental changes within paleobasin against the background of relative cooling during the OAE 2. At the same time, oxygen isotope ratios indicate a relative warming or desalination of the basin. Proceeding from the general significant impoverishment of nannofossil assemblages in this interval and increased abundance of species resistant to such environmental changes (*Watznaueria* spp.), the warming seems possible in some areas.

(5) The formation of elementary cyclites correlates with the Milankovitch precession cycles (~21 ka). The number of cyclites in different intervals suggests that the duration of periods corresponding to the accumu-

lation of OM-rich sediments was 230–250 ka, whereas the entire OAE 2 sequence was accumulated in ~370–410 ka. The formation of the whole sedimentary cycle, which comprises all OAE 2 sediments, likely corresponds to a single eccentricity cycle ~400 ka long. This statement is consistent with the estimate based on precession cycles.

(6) The lithological and geochemical properties of OM-rich sediments imply that the anoxic environment in the basin during their deposition was intermittent and involved an insignificant part of the water column (mostly, bottom water layers). Anoxia did not play any significant role in the accumulation of organic matter in sediments.

(7) OM-rich sediments were deposited against the background of a rapid eustatic transgression, when basin waters were highly enriched with biophile elements transported from coastal landscapes, which stimulated the rapid growth in productivity of phyto- and bacterioplankton and the accumulation of high amount of OM in sediments. The nonlinear development of the transgression resulted in the irregular influx of biophile elements to the basin, which affected the formation of cyclic sequences.

ACKNOWLEDGMENTS

This work was supported by the Russian Foundation for Basic Research (project no. 12-05-01138) and the Presidium of the Russian Academy of Sciences (program no. 27).

REFERENCES

Alekseev, A.S., Kopaevich, L.F., Vengertsev, V.V., and Kuz'micheva, T.A., Lithology and micropaleontology of the Cenomanian/Turonian boundary sediments in the southwestern Crimea, in *Ocherki geologii Kryma* (Essays on the Crimean Geology), Moscow: MGU, 1997, issue 1, pp. 54–73.

Arndt, S., Brumsack, H.-J., and Wirtz, K.W., Cretaceous black shales as active bioreactor: A biogeochemical model for the deep biosphere encountered during ODP Leg 207 (Demerara Rise), *Geochim. Cosmochim. Acta*, 2006, vol. 70, pp. 408–425.

Arthur, M.A. and Schlanger, S.O., Cretaceous "oceanic anoxic events" as causal factors in development of reef-reservoired giant oil fields, *Bull. Am. Assoc. Pet. Geol.*, 1979, vol. 63, pp. 870–885.

Arthur, M.A., Schlanger, S.O., and Jenkyns, H.C., The Cenomanian-Turonian oceanic anoxic event: II. Paleoceanographic controls on organic matter production and preservation, in *Marine Petroleum Source Rocks*, London: Geol. Soc. Spec. Publ., 1987, vol. 26, pp. 401–420.

Arthur, M.A., Dean, W.E., and Pratt, L.M., Geochemical and climatic effects of increased marine organic carbon burial at the Cenomanian/Turonian boundary, *Nature*, 1988, vol. 335, pp. 714–717.

Arthur, M.A., Jenkyns, H.C., Brumsack, H.-J., and Schlanger, S.O., Stratigraphy, geochemistry, and paleoceanography of organic carbon-rich Cretaceous sequences, in *Cretaceous Resources, Events and Rhythms*, Ginsburg, R.N., Beaudoin, B, Eds., Dordrecht: Kluwer Acad. Publ., 1990, pp. 75–119.

Bowman, A.R. and Bralower, T.J., *Paleoceanographic* significance of high-resolution carbon isotope records across the Cenomanian-Turonian boundary in the Western Interior and New Jersey coastal plain, USA, *Mar. Geol.*, 2005, vol. 217, pp. 305–321.

Bragina, L.G., Cenomanian–Turonian radiolarians in the Mountainous Crimea, *Byull. Mosk. O-va Ispyt. Prir., Otd. Geol.*, 1999, vol. 74, no. 3, pp. 43–50.

Bralower, T.J., Fullagar, P.D., Paull, C.K., et al., Mid-Cretaceous strontium-isotope stratigraphy of deep-sea sections, *Geol. Soc. Am. Bull.*, 1997, vol. 109, no. 10, pp. 1421–1442.

Brumsack, H.-J., Geochemistry of Cretaceous black shales from the Atlantic Ocean (DSDP Leg 11, 14, 36 and 41), *Chem. Geol.*, 1980, vol. 31, pp. 1–25.

Brumsack, H.-J., The inorganic geochemistry of cretaceous black shales (DSDP Leg 41) in comparison to modern upwelling sediments from the Gulf of California and the Black Sea, *Geol. Rundsch.*, 1986, vol. 78, pp. 851–882.

Brumsack, H.-J., The trace metal content of recent organic carbon-rich sediments: Implication for Cretaceous black shale formation, *Palaeogeogr., Palaeoclimatol., Palaeoecol.*, 2006, vol. 232, pp. 344–361.

Burnett, J., Upper Cretaceous, in *Calcareous Nannofossil Biostratigraphy,* Bown, P. R., Ed., Cambridge: Univ. Press, 1998, pp. 132–199.

Caron, M., Robaszynski, F., Amedro, F., et al., Estimation de la duree de l'evenement anoxique global au passage Cenomanien/Turonien; approche cyclostratigraphique dans la formation Bahloul en Tunisie central, *Bull. Soc. Geol. Fr.,* 1999, vol. 170, no. 2, pp. 145–160.

Čech, S., Hradecka, L., Svobodova, M., and Švabenicka, L., Cenomanian and Cenomanian-Turonian boundary in the southern part of the Bohemian Cretaceous basin, Czech Republic, *Bull. Geosci.*, 2005, vol. 80, no. 4, pp. 321–354.

Dymond, J., Suess, T., and Lyle, M., Barium in deep-sea sediment: A geochemical proxy for paleoproductivity, *Paleoceanography*, 1992, vol. 7, pp. 163–181.

El-Sabbagh, A., Tantawy, A.A., Keller, G., et al., Stratigraphy of the Cenomanian-Turonian oceanic anoxic event OAE 2 in shallow shelf sequences of NE Egypt, *Cretaceous. Res*. 2011, vol. 32, no. 6, pp. 705–722.

Erba, E., Calcareous nannofossils and Mesozoic oceanic anoxic events, *Mar. Micropaleontol.*, 2004, vol. 52, pp. 85–106.

Falkner, K.K., Klinkhammer, G.P., Bowers, T.S., et al., The behavior of barium in anoxic marine waters, *Geochim. Cosmochim. Acta*, 1993, vol. 57, no. 3, pp. 537–554.

Fernando, A.G.S., Takashima, R., Nishi, H., et al., Calcareous nannofossil biostratigraphy of the Thomel Level (OAE 2) in the Lambruisse section, Vocontian basin, southeast France, *Geobios*, 2010, vol. 43, pp. 45–57.

Fernando, A.G.S., Nishi, H., Tanabe, K., et al., Calcareous nannofossil biostratigraphic study of forearc basin sediments: Lower to Upper Cretaceous Budden Canyon Formation (Great Valley Group), northern California, USA, *Island Arc*, 2011, doi: 10.1111/j.1440-1738.2011.00770.

Fisher, J.K., Price, G.D., Hart, M.B., and Leng, M.J., Stable isotope analysis of the Cenomanian-Turonian (Late

Cretaceous) oceanic anoxic event of the Crimea, *Cretaceous Res*. 2005, vol. 26, no. 6, pp. 853–863.

Gale, A.S., Young, J.R., Shackleton, N.J., et al., Orbital tuning of Cenomanian marly chalk succession: Towards a Milankovich time-scale for the Late Cretaceous, *Philos. Trans. R. Soc. London*, 1999, vol. 357, no. 1757, pp. 1815–1829.

Gale, A.S., Smith, A.B., Monks, N.E.A., et al., Marine biodiversity through the late Cenomanian-early Turonian: Paleoceanographic control and sequence stratigraphic biases, *J. Geol. Soc. London,* 2000, vol. 157, pp. 745–75.

Gale, A.S., Hardenbol, J., Hathway, B., et al., Global correlation of Cenomanian (Upper Cretaceous) sequences: Evidence for Milankovitch control on sea level, *Geology*, 2002, vol. 30, no. 4, pp. 291–294.

Gavrilov, Yu.O., Possible causes for the accumulation of organic-rich sediments in connection with eustatic sealevel fluctuations, in *Ekosistemnye perestroiki i evolyutsiya biosfery* (Ecosystem Rearrangements and Evolution of the Biosphere), Rozanov, A.Yu., Semikhatov, M.A., Eds., Moscow: Nedra, 1994, issue 1, pp. 305–311.

Gavrilov, Yu.O. and Kopaevich, L.F., Geochemical, biochemical, and biotic consequences of eustatic fluctuations, *Stratigr. Geol. Correlation*, 1996, no. 4, pp. 3–14.

Gavrilov, Yu.O. and Shcherbinina, E.A., Global biospheric event at the Paleocene/Eocene boundary, in *Sovremennye problemy geologii* (Recent Problems of Geology), Gavrilov, Yu.O. and Khutorskoi, M.D., Eds., Moscow: Nauka, 2004.

Gavrilov, Yu.O. and Shcherbinina, E.A., Mid-Cretaceous Anoxic Events in the Eastern Caucasus, Russia, *7th Int. Symp. on the Cretaceous. Scientific Program and Abstracts*, 2005, pp. 90–91

Gavrilov, Yu.O., Shcherbinina, E.A., and Oberhänsli, H., Paleocene/Eocene boundary events in the Northeastern Peri-Tethys, in *Causes and Consequences of Globally Warm Climates in the Early Paleogene*, Wing, S.L., Gingerich, P.D., and Schmitz, B., Thomas, E., Eds., Colorado: Geol. Soc. Am. Spec. Pap. 369, 2003, pp. 147–168.

Gavrilov, Yu.O., Shcherbinina, E.A., and Cherkashin, V.I., Reflection of Mesozoic and Cenozoic global and interregional events in sedimentary complexes of the northeastern Caucasus (Dagestan), in *Geologiya i mineral'no-syr'evye resursy Yuzhnogo federal'nogo okruga* (Geology and Raw Mineral Resources in the Southern Federal District, Cherkashin, V.I., Ed., Makhachkala, 2006, pp. 15–24.

Gavrilov, Yu.O., Kodina, L.A., Lubchenko, I.Yu., and Muzylev, N.G., Late Paleocene anoxic event in epicontinental seas of the Peri-Tethys and formation of the sapropelite horizon: Sedimentology and geochemistry, *Lithol. Miner. Resour.*, 1997, no. 5, pp. 483–507.

Gavrilov, Yu.O., Shchepetova, E.V., Baraboshkin, E.Yu., and Shcherbinina, E.A., Early Cretaceous anoxic basin in the Russian Plate: Sedimentology and geochemistry, *Lithol. Miner. Resour.*, 2002, no. 4, pp. 345–365.

Gavrilov, Yu.O., Shcherbinina, E.A., Golovanova, O.V., and Pokrovskii, B.G., Late Cenomanian anoxic event (OAE 2) in the Aimaki section in Mountainous Dagestan, *Byull. Mosk. O-va Ispyt. Prir., Otd. Geol.*, 2009, vol. 84, no. 2, pp. 94–108.

Geologiya SSSR. Armyanskaya SSR. Geologicheskoe opisanie (Geology of the USSR: Armenian SSR. Geological Description), Moscow: Nedra, 1970, vol. 53.

Geologiya SSSR. Azerbaidzhanskaya SSR. Geologicheskoe opisanie (Geology of the USSR: Azerbaijan SSR. Geological Description), Moscow: Nedra, 1972, vol. 57.

Ginzburg, A.I., *Atlas petrograficheskikh tipov goryuchikh slantsev* (Atlas of Petrographic Types of Bituminous Shales), Leningrad: Nedra, 1991.

Goldberg, E.D. and Arrhenius, G.O.S., Chemistry of Pacific pelagic sediments, *Geochim. Cosmochim. Acta*, 1958, vol. 13, no. 2-3, pp. 153–212.

Hardas, P. and Mutterlose, J., Calcareous nannofossil biostratigraphy of the Cenomanian/Turonian boundary interval of ODP Leg 207 Demerara Rise, *Micropaleontology*, 2006, vol. 49, pp. 165–179.

Hardas, P. and Mutterlose, J., Calcareous nannofossil assemblages of oceanic anoxic event 2 in the equatorial Atlantic: Evidence of eutrophication event, *Mar. Micropaleontol.*, 2007, vol. 66, pp. 52–69.

Hasegawa, T., Cenomanian-Turonian carbon isotope events recorded in terrestrial organic matter from northern Japan, *Palaeogeogr., Palaeoclimatol., Palaeoecol.*, 1997, vol. 130, pp. 251–273.

Hays, J.D. and Pittman, W.C., Lithospheric plate motion, sea level changes and climatic and ecological consequences, *Nature*, 1973, vol. 246, pp. 18–22.

Henkel, S., Mogollon, J.M., Nothen, K., et al., Diagenetic barium cycling in black sea sediments - a case study for anoxic marine environments, *Geochim. Cosmochim. Acta*, 2012, vol. 88, pp. 88–105.

Jarvis, I., Murphy, A.M., and Gale, A.S., Geochemistry of pelagic and hemipelagic carbonates: Criteria for identifying systems tracts and sea-level change, *J. Geol. Soc. London*, 2001, vol. 158, pp. 685–696.

Jarvis, I., Mabrouk, A., Moody, R.T.J., et al., Applications of carbon isotope and elemental (Sr/Ca,Mn) chemostratigraphy to sequence analysis: Sea-level change and the global correlation of pelagic carbonates, in *The Geology of East Libya,* Salem, M.J., El-Hawat, A.S, Eds., Tripoli: Earth Sci. Soc. Libya, 2008, vol. 1, pp. 369–396.

Jarvis, I., Lignum, J.S., Gröcke, D.R., Jenkyns, H. C., and Pearce, M. A., Black shale deposition, atmospheric CO_2 drawdown and cooling during the Cenomanian-Turonian oceanic anoxic event, *Paleoceanography*, 2011, vol. 26, PA3201, doi: 10.1029/2010pa002081.

Jenkyns, H.C., Cretaceous anoxic events: From continents to oceans, *J. Geol. Soc. London*, 1980, vol. 137, pp. 171–188.

Kasten, S., Haese, R.R., Zabel, M., et al., Barium peaks at glacial terminations in sediments of the equatorial Atlantic ocean—relicts of deglacial productivity pulses?, *Chem. Geol.*, 2001, vol. 175, no. 3–4, pp. 635–651.

Keller, G., Berner, Z., Adatte, T., and Stueben, D., Cenomanian-Turonian and $\delta^{13}C$, and $\delta^{18}O$, sea level and salinity variations at Pueblo, Colorado, *Palaeogeogr., Palaeoclimatol., Palaeoecol.*, 2004, vol. 211, no. 1–2, pp. 19–43.

Kennedy, W.J., Walaszczyk, I., and Cobban, W.A., The global boundary stratotype section and point for the base of the Turonian stage of the Cretaceous: Pueblo, Colorado, U.S.A., *Episodes*, 2005, vol. 28, no. 2, pp. 93–104.

Kerr, A.C., Oceanic plateau formation: A cause of mass extinction and black shale deposition around the Cenomanian-Turonian boundary?, *J. Geol. Soc. London*, 1998, vol. 155, pp. 619–626.

Kopaevich, L. and Kuzmicheva, T., The Cenomanian-Turonian boundary in southwestern Crimea, Ukraine: Foraminifera and palaeogeographic implications, in *Aspects of Cretaceous Stratigraphy and Palaeobiogeography*, Wagreich, M., Ed., *Proc. of the 6th International Cretaceous Symposium,* Vienna: Osterreich. Akad. Wissensch., 2002, vol. 15, pp. 129–149.

Kuhnt, W., Nederbragt, S., and Leine, L., Cyclicity of Cenomanian-Turonian organic-carbon-rich sediments in the Tarfaya Atlantic Coastal Basin (Morocco), *Cretaceous Res.*, 1997, vol. 18, no. 4, pp. 587–601.

Kuhnt, W., Luderer, F., and Nederbragt, S., Orbital-scale record of the late Cenomanian-Turonian oceanic anoxic event (OAE-2) in the Tarfaya Basin (Morocco), *Int. Earth Sci. (Geol. Rundsch.)*, 2005, vol. 94, pp. 147–159.

Kuroda, J., Ogawa, N.O., Tanimizu, M., et al., Contemporaneous massive subaerial volcanism and Late Cretaceous oceanic anoxic event 2, *Earth Planet. Sci. Lett.*, 2007, vol. 256, pp. 211–223.

Kuz'micheva, T.A., Distribution of foramifers in the Cenomanian? / Turonian boundary rocks in the Mt. Belaya section (southwestern Crimea, Ukraine), Vestn. MGU, Ser. 4, pp. 27–35.

Lamolda, M.A., Gorostidi, A., Martinez, R., et al., Fossil occurrences in the upper Cenomanian-lower Turonian at Ganuza, northern Spain: An approach to Cenomanian/Turonian boundary chronostratigraphy, *Cretaceous Res.*, 1997, vol. 18, pp. 331–353.

Levitan, M.A., Alekseev, A.S., Badulina, N.V., et al., Geochemistry of Cenomanian/Turonian boundary sediments in the mountainous part of Crimea and the northwestern Caucasus, *Geochem. Int.*, 2010, vol. 48, no. 6, pp. 534–554.

Linnert, C., Mutterlose, J., and Erbacher, J., Calcareous nannofossils of the Cenomanian/Turonian boundary interval from the boreal realm (Wunstorf, northwest Germany), *Mar. Micropaleontol.*, 2010, vol. 74, pp. 38–58.

Lopatin, N.V. and Emets, T.P., *Piroliz v neftegazovoi geokhimii* (Pyrolysis in Petroleum Geology), Moscow: Nauka, 1987.

Luciani, V. and Cobianchi, M., The Bonarelli Level and other black shales in the Cenomanian-Turonian of the northeastern dolomites (Italy): Calcareous nannofossil and foraminiferal data, *Cretaceous Res.*, 1999, vol. 20, pp. 135–167.

McManus, J., Berelson, W.M., Klinkhammer, G.P., et al., Geochemistry of barium in marine sediments: Implications for its use as a paleoproxy, *Geochim. Cosmochim. Acta*, 1998, vol. 62, no. 21–22, pp. 3453–3473.

Melinte-Dobrinescu, M.C. and Bojar, A.-V., Biostratigraphic and isotopic record of the Cenomanian-Turonian deposits in the Ohaba-Ponor section (SW Haţeg, Romania), *Cretaceous Res.*, 2008, vol. 29, pp. 1024–1034.

Metody izucheniya osadochnykh porod (Methods for the Study of Sedimentary Rocks), Moscow: Gosgeoltekhizdat, 1957, vol. 2.

Naidin, D.P., Late Mesozoic events in the eastern European paleobiogeographic zone: Communication 2. The Cenomanian/Turonian and Maestrichtian/Danian boundary events, *Byull. Mosk. O-va Ispyt. Prir., Otd. Geol.*, 1993, vol. 68, no. 3, pp. 33–53.

Naidin, D.P. and Alekseev, A.S., The Cenomanian section in the Kachi and Bodrak interfluve area (Crimea), *Izv. Vyssh. Uchebn. Zaved., Geol. Razved.*, 1980, no. 4, pp. 11–25.

Naidin, D.P. and Kiyashko, S.I., Geochemical characteristics of the Cenomanian/Turonian boundary sediments in the Mountainous Crimea: Communication 1. Lithological composition, contents of organic carbon and some elements, *Byull. Mosk. O-va Ispyt. Prir., Otd. Geol.*, 1994a, vol. 69, no.1, pp. 28–42.

Naidin, D.P. and Kiyashko, S.I., Geochemical characteristics of the Cenomanian/Turonian boundary sediments in the Mountainous Crimea: Communication 2. Isotopic composition and content of oxygen; conditions of organic carbon accumulation, *Byull. Mosk. O-va Ispyt. Prir., Otd. Geol.*, 1994b, vol. 69, no. 2, pp. 59–74.

Paul, C.R.C., Lamolda, M.A., Mitchell, S.F., et al., The Cenomanian-Turonian boundary at Eastburne (Sussex, UK): A proposed European reference section, *Palaeogeogr., Palaeoclimatol., Palaeoecol.*, 1999, vol. 150, pp. 83–121.

Paytan, A. and Griffith, E.M., Marine barite: Recorder of variations in ocean export productivity, *Deep Sea Res. Part II-Topical Studies in Oceanography*, 2007, vol. 54, pp. 687–705.

Perch-Nielsen, K., Mesozoic calcareous nannofossil, in *Plankton Stratigraphy. 1. Planktic Foraminifera, Calcareous Nannofossils and Calpionellids*, Bolli, H.M, Saunders, J.B., and Perch-Nielsen, K, Eds., 1985, pp. 329–426.

Pfeifer, K., Kasten, S., Hensen, C., and Schulz, H.D., Reconstruction of primary productivity from the barium contents in surface sediments of the South Atlantic Ocean, *Mar. Geol.*, 2001, vol. 177, pp. 13–24.

Prokoph, A., Villeneuve, M., Agterberg, F.P., and Rachold, V., Geochronology and calibration of global Milankovitch cyclicity at the Cenomanian-Turonian boundary, *Geology*, 2001, vol. 29, no. 6, pp. 523–526.

Robaszynski, F., Gale, A.S., Juignet, P., et al., Sequence stratigraphy in the Upper Cretaceous series of the Anglo-Paris Basin: Exemplified by the Cenomanian stage, in *Mesozoic and Cenozoic Sequence Stratigraphy of European Basins*, Graciansky, P.C., Hardenbol, J., Jacquin, T, et al., Eds., SEPM Spec. Publ., 1998, vol. 60, pp. 363–386.

Sageman, B.B., Rich, J., Arthur, M.A., Birchfield, G.E., and Dean, W.E., Evidence for Milankovitch periodicities in Cenomanian-Turonian lithological and geochemical cycles, Western Interior USA, *J. Sediment. Res.*, 1997, vol. 67, pp. 286–302.

Sageman, B.B., Meyers, S.R., and Arthur, M.A., Orbital time scale and new C-isotope record for Cenomanian-Turonian boundary stratotype, *Geology*, 2006, vol. 34, no. 2, pp. 125–128.

Schlanger, S.O. and Jenkyns, H.C., Cretaceous oceanic anoxic events: Causes and consequences, *Geol. Mijnbow*, 1976, vol. 55, pp. 179–184.

Schlanger, S.O., Arthur, M.A., Jenkyns, H.C., and Scholle, P.A., The Cenomanian-Turonian oceanic anoxic event, I. Stratigraphy and distribution of organic carbon-rich beds and marine $\delta^{13}C$ excursion, *Geol. Soc. London Spec. Publ.,* 1987, vol. 26, pp. 371–399.

Schmitz, B., Barium, equatorial high productivity, and the northward wandering of the Indian continent, *Paleoceanography*, 1987, vol. 2, pp. 63–78.

Scopelliti, G., Bellanca, A., Coccioni, R., Luciani, V., et al., High-resolution geochemical and biotic records of the Tethyan 'Bonarelli Level' (OAE 2, latest Cenomanian) from the Calabianca-Guidaloca composite section, northwestern Sicily, Italy, *Palaeogeogr., Palaeoclimatol., Palaeoecol.*, 2004, vol. 208, pp. 293 – 317.

Shamrock, J. and Watkins, D.K., Evolution of the Cretaceous calcareous nanofossil genus *Eiffelithus* and its biostratigraphic significance, *Cretaceous Res.*, 2009, vol. 30, pp. 1083–1102.

Shcherbinina, E.A. and Gavrilov, Yu.O., Stratigraphy of Cretaceous and Lower Paleogene sediments in central Dagestan based on nannoplankton, in *Regional'naya geologiya i neftegazonosnost' Kavkaza* (Regional Geology and Petroleum Potential of Caucasus), Cherkashin, V.I., Ed., Makhachkala, 2012, pp. 57–65.

Shcherbinina, E. and Aleksandrova, G., Nannofossil and dinocyst record across the Cenomanian/Turonian transition of the Crimea, Ukraine, *7th Int. Symp. on the Cretaceous, Scientific Program and Abstracts*, Neuchatel, 2005, pp. 200–201.

Shcherbinina, E.A., Gavrilov, Yu.O., Golovanova, O.V., and Pokrovskii, B.G., Paleoecological rearrangements during the Cretaceous anoxic events in the Dagestan sector of the East Caucasian basin, in *Geologiya i poleznye iskopaemye Kavkaza* (Geology and Mineral Resources of the Caucasus), Cherkashin, V.I., Ed., Makhachkala, 2011, pp. 53–59.

Sinninghe, Damsté J.S., van Bentum, E.C., Reichart, G.-J., A CO_2 decrease-driven cooling and increased latitudinal temperature gradient during the mid-Cretaceous Oceanic Anoxic Event 2, *Earth Planet. Sci. Lett.*, 2010, vol. 293, pp. 97–103.

Sinton, C.W. and Duncan, R.A., Potential links between ocean plateau volcanism and global ocean anoxia at the Cenomanian-Turonian boundary, *Econ. Geol.*, 1997, vol. 92, pp. 836–842.

Sissingh, W., Biostratigraphy of Cretaceous calcareous nannoplankton, *Geol. Mijnbouw*, 1977, vol. 56, pp. 37–65.

Snow, L.J., Duncan, R.A., and Bralower, T.J., Trace element abundances in the Rock Canyon Anticline, Pueblo, Colorado, marine sedimentary section and their relationship to Caribbean plateau construction and oxygen anoxic event 2, *Paleoceanography*, 2005, vol. 20, p. A3005, doi:10.1029/2004PA001093.

Tantawy, A.A., Calcareous nannofossil biostratigraphy and paleoecology of the Cenomanian-Turonian transition in the Tarfaya Basin, southern Morocco, *Cretaceous Res.*, 2008, vol. 29, no. 5-6, pp. 995–1007.

Torres, M.E., Brumsack, H.-J., Bohrmann, G., and Emeis, K.-C., Barite fronts in continental margin sediments: A new look at barium remobilization in the zone of sulfate reduction and formation of heavy barites in diagenetic fronts, *Chem. Geol.*, 1996, vol. 127, pp. 125–139.

Tremolada, F., Erba, E., van de Schootbrugge, B., and Mattioli, E., Calcareous nannofossil changes during the late Callovian-early Oxfordian cooling phase, *Mar. Micropaleontol.*, 2006, vol. 59, pp. 197–209.

Tsikos, H., Jenkyns, H.C., Walsworth-Bell, B., et al., Carbon-isotope stratigraphy recorded by the Cenomanian-Turonian oceanic anoxic event: Correlation and implications based on three key localities, J. Geol. Soc. London, 2004, vol. 161, pp. 711–719.

Tur, N.A., Planktonic foraminifera recovery from the Cenomanian-Turonian mass extinction event, northeastern Caucasus, in Biotic Recovery from Mass Extinction Events, *Geol. Soc. London. Spec. Publ.*, 1996, no. 102, pp. 259–264.

Turgeon, S. and Brumsack, H.-J., Anoxic, vs dysoxic events recorded in sediment geochemistry during the Cenomanian-Turonian Boundary Event (Cretaceous) in the Umbria-Marche Basin of central Italy, *Chem. Geol.*, 2006, vol. 234, pp. 321–339.

Voigt, S., Gale, A.S., and Voigt, T., Sea-level change, carbon cycling and palaeoclimate during the late Cenomanian of northwest Europe; an integrated palaeoenvironmental analysis, *Cretaceous Res.*, 2006, vol. 27, pp. 836–858.

von Breymann, M.T., Emeis, K.-C., and Suess, E., Water depth and diagenetic constraints on the use of barium as a palaeoproductivity indicator, in *Upwelling Systems: Evolution since the Early Miocene*, Summerhayes, C.P., Prell, E.L., and Emeis, K.-C, Eds., Geol. Soc. Spec. Publ., 1992, vol. 64, pp. 131–145.

Waslworth-Bell, B. and Erba, E., and C/T Net-Group, Calcareous nannofossils and the Cenomanian/Turonian OAE2, *Geophys. Res. Abstr.*, 2003, vol. 5, no. 06084.

Weissert, H. and Erba, E., Volcanism, CO_2 and palaeoclimate: A Late Jurassic-Early Cretaceous carbon and oxygen isotope record, *J. Geol. Soc. London*, 2004, vol. 161, pp. 1–8.

Westermann, S., Fiet, N., Fleitmann, D., et al., Absence of anoxic conditions during OAE 2 in Helvetic realm?, *Geophys. Res. Abstr.*, 2008, vol. 10, no. A-08484.

Wilmsen, M., Sequence stratigraphy and palaeoceanography of the Cenomanian stage in northern Germany, *Cretaceous Res.*, 2003, vol. 24, pp. 525–568.

Yazykova, E. and Zonova, T., Upper Cretaceous stable carbon isotope stratigraphy of terrestrial organic matter from Sakhalin, Russian Far East: A proxy for the isotopic composition of paleoatmospheric CO_2 by T. Hasegava et al. - Discussion, *Palaeogeogr., Palaeoclimatol., Palaeoecol.*, 2004, vol. 215, pp. 173–177.

Translated by I. Basov